The Anomalous Thermal Properties of Glasses at Low Temperatures*

R. O. Pohl, Cornell University, Ithaca, N. Y. 14853

and

G. L. Salinger, Rensselaer Polytechnic Institute, Troy, N. Y. 12181

In the past several years there has been an intensive effort to understand the properties of amorphous dielectrics below 1 K. At these low temperatures thermal phenomena should be dominated by the properties of long wave length elastic waves which are well understood. Wavelengths λ of thermal vibrations can be found from $h\nu = kT$ and $\nu\lambda = v$ where v, the sound velocity is a few thousand meters per second. Thus below 1 K, $\lambda \sim 1000$ Å. Since this is much larger than microscopic disorder there should be little difference between the thermal properties of amorphous and crystalline dielectrics. Experimentally there is great regularity in the behavior of a particular thermal property for all amorphous dielectrics; but this behavior is very different than that for crystalline dielectrics. For example, the specific heat c of amorphous dielectrics plotted as c/T vs T^2 is shown in Fig. 1 below 0.7 K. In general the specific heat c can be fit to

$$c = c_1 T + c_3 T^3 \qquad (1)$$

where $c_1 = 1 - 5 \times 10^{-6}$ J gm^{-1} K^{-2} and c_3 is larger than is expected from acoustic measurements. The thermal conductivity Λ of a variety of amorphous dielectrics as a function of temperature[1,2] is shown on Fig. 2. Below 1 K,

$$\Lambda = AT^{\delta} \qquad (2)$$

where $\delta = 1.9 \pm .1$ and $A = 3 \times 10^{-4}$ W cm^{-1} K^{-1} within a factor of three for all the materials. Around 10 K, there is a plateau where $\Lambda = 10^{-3}$ W cm^{-1} K^{-1} within a factor of 2 for all substances. This is in marked contrast to

DISCLAIMER

the behavior of crystalline dielectrics which follow a T^3 dependence below 1 K and the addition of a few parts per million of an impurity decreases the thermal conductivity by two orders of magnitude.[3]

Anomalous behavior has also been noted for amorphous dielectrics in measurements of acoustic attenuation[4] and velocity[5], dielectric constant[6], thermal expansion[7], nuclear magnetic resonance[8] and optical properties.[9]

A number of models have been proposed to explain these results.[10] We will concentrate on one which invokes systems having very few levels.[11] The connection between these systems and the nature of the glassy state is not known.

In this paper we show that (a) specific heat measurements above 0.1 K indicate a distribution of local modes independent of energy; (b) ultrasonic attenuation measurements at low powers indicate that the local mode systems can have at most a few levels; (c) ultrasonic velocity measurements give information about phonon-local mode coupling parameters; (d) the measured thermal conductivity agrees with that calculated from the above information assuming that the energy independent distribution of modes observed in the specific heat is responsible for phonon scattering; (e) thermal expansion and far infrared experiments indicate a phonon assisted tunneling model; (f) several experiments, however, indicate that the modes observed in the specific heat measurements may not all scatter phonons.

SPECIFIC HEAT

The specific heat of a solid is calculated from the temperature derivative of the internal energy which can be expressed as an integral of the product of the energy ε of the mode contributing, the number of such modes per unit energy $n(\varepsilon)$, the probability that the mode is occupied $f(\varepsilon/kT)$:

$$U = \int_0^{\varepsilon_m} \varepsilon\, n(\varepsilon)\, f(\varepsilon/kT)\, d\varepsilon \qquad (3)$$

The upper limit of integration is usually determined by the condition that the sum of the density of states is the total number of those modes $\mathcal{N}$ in the solid

$$\mathcal{N} = \int_0^{\varepsilon_m} n(\varepsilon) d\varepsilon \qquad (4)$$

However since the distribution functions approach zero rapidly when $kT \ll \varepsilon$, little error is made in replacing ε_m by infinity in Eq. 3 when the low temperature behavior is of interest. Thus

$$U = (kT)^2 \int_0^{\infty} n(\varepsilon)\, x\, f(x) dx, \qquad (5)$$

where $x = \varepsilon/kT$. If

$$n(\varepsilon) = \sum n_q \varepsilon^q \qquad (6)$$

the low temperature dependence of U depends on T^{2+q} and the specific heat is proportional to T^{1+q} since $c \propto dU/dT$.

The specific heats of solids below room temperature have been explained by the Debye theory[12] in which the theory for blackbody radiation developed by Planck is applied to elastic waves in homogeneous isotropic solids not necessarily crystals. The number of states per unit energy is proportional to ε^2 so that at low temperatures when the wavelength of the elastic wave is much longer than the microscope disorder of the material, the specific heat c depends upon the absolute temperature cubed

$$\frac{c}{T^3} = c_{3,D} = \frac{16\pi^5 k^4}{5h^3} \frac{1}{\rho v^3}, \qquad (7)$$

where ρ is the density of the material and v is an average velocity of sound

$$\frac{1}{v^3} = \frac{1}{3}\left(\frac{1}{v_{\ell}{}^3} + \frac{2}{v_t{}^3}\right). \qquad (8)$$

Here ℓ and t refer to the longitudinal and transverse polarizations respectively. As shown, below 1 K, $\lambda > 1000$ A; thus the specific heat of any material should be proportional to T^3 below 1 K, the magnitude depends upon the velocity of sound and the density of the material. We have avoided the common formulation using the Debye temperature θ because of ambiguities in defining θ for polyatomic noncrystalline solids.[13]

A plot of c/T^3 versus T is shown on Fig. 3 for crystalline quartz. The results are typical for a large variety of crystalline materials, in which the calorimetrically measured specific heat is accurately determined by sound velocity measurements through Eq. 7. For crystalline quartz[14] $c/T^3 = 5.5 \times 10^{-7}$ W s gm^{-1} K^{-4} and $\bar{v} = 4.4 \times 10^5$ cm s^{-1}.

Data for the specific heat of vitreous silica[15], also plotted on Fig. 3, are typical for a great variety of amorphous solids. Above 1 K, c/T^3 has a hump which was attributed to discrete oscillations which could be identified from prominent peaks in the Raman spectrum.[15] More recently the specific heat of crystobolite[16], a crystalline form of silica, was found to vary in the same way as vitreous silica. Neutron diffraction studies show a low frequency transverse acoustic mode.[17] In analogy with the more complex neutron diffraction and specific heat studies of GeO_2,[16] it is argued that the hump in c/T^3 above 1 K is due to a modification of the crystalline density of states. An indication of the universality of an increased density of low frequency states in amorphous solids comes from electron tunneling experiments in amorphous metal films.[10] There is much interesting science to be learned in trying to explain the hump in c/T^3 above 1 K, and to correlate it with data on thermal expansion,

internal friction, dielectric constant, nuclear magnetic resonance and optical spectroscopy experiments. However, we turn out attention to the temperature range below 1 K.

Below 1 K the deviation of the specific heat from the Debye value increases until below 0.2 K the calorimetrically measured specific heat is more than an order of magnitude greater than the Debye prediction. As shown in Fig. 1 these data are typical for all amorphous materials and can be described in Eq. 1 with $c_3 > c_{3,D}$. Thus as shown in Fig. 4 from Eq. 6

$$n(\varepsilon) = n_o + (n_2' + n_{2,D})\varepsilon^2 \qquad (9)$$

where $n_{2,D}$ is the Debye distribution of states. The coefficient n_o implies that some number of states per unit energy is independent of energy. The value for n_o depends upon the model chosen but seems to have a value in the range of $4 - 25 \times 10^{32}$ erg^{-1} cm^{-3} or about 10^{17} cm^{-3} up to 1.5 K.

The models to explain these effects fall into two classes. One depends on lack of long range order mainly through variations in density.[10] These models are attractive because a crystalline solid should have a more uniform density than an amorphous one. However, the theories usually involve parameters which are not easily experimentally accessible. The other group of models invoke a distribution of localized modes.[10] Of these the one receiving the most attention is the phonon-assisted tunneling model.[11] In this model it is assumed that because of the morphology of the system a group of atoms may have more than one equilibrium position which does not necessarily significantly increase the internal energy of the system. At low temperature the atoms do not have enough energy to surmount the barriers

between configurations and they tunnel from one configuration to the other with the small energy difference made up by lattice vibrations. In its simplest form one can ignore the tunneling aspect of the model and just assume a local density of modes having a few discrete levels. Evidence for this model comes from ultrasonic attenuation experiments.

ULTRASONIC EXPERIMENTS

The attenuation of gigahertz sound waves is plotted in Fig. 5 as a function of power level parametrized by frequency.[4] At very low powers the attenuation is constant. As the power is increased over a few orders of magnitude the attenuation decreases and the mean free path increases by an order of magnitude. This decrease in attenuation can be explained[11] if the local modes are assumed to consist of very few levels so that at higher powers the populations of the levels can be equalized leading to no net energy removed from the ultrasonic wave. Thus the mean free path increases. This is the same process as saturating a nuclear magnetic resonance signal.

The calculation for the acoustic attenuation of phonons resonantly scattered by local mode systems is very similar to the calculation of resonance absorption in the case of dielectric or anelastic relaxation. In our case, at low powers, the acoustic beam causes periodic deformations of the two level system which perturbs the energy of the system. (For ease a two level system is considered rather that a few level system.) The periodic perturbation causes transitions as outlined in quantum mechanics:[18]

$$\tau^{-1} = \frac{2\pi}{\hbar^2} |H_{ij}|^2 \rho(\omega). \qquad (10)$$

The matrix element is given by:

$$H_{ij} = \left(\frac{\hbar\omega}{2\rho c^2}\right)^{\frac{1}{2}} M, \tag{11}$$

where M is the coupling energy between the phonon and the two level system. The density of available states $\rho(\omega)$ for a two level system is $n_o \tanh \frac{h\omega}{2kT}$. The inverse mean free path is $\ell^{-1} = (\tau v)^{-1}$ so that

$$\ell_\nu^{-1} = \frac{\pi n_o M_\nu^2}{\rho v_\nu} \omega \tanh \frac{\hbar\omega}{2kT} . \tag{12}$$

where the subscript ν refers to the polarization of the sound wave. Even at these low temperatures for gigahertz ultrasonic experiments $h\omega << kT$ so that $\ell^{-1} \propto \frac{\omega^2}{T}$. The ω^2 dependence is seen in Fig. 5 and in Fig. 6 we see that $\ell_\nu^{-1} \propto T^{-0.7}$ at low temperatures and only for power levels below 10^{-7} W/cm^2.

The above discussion assumes that the occupation number of the levels is independent of the sound wave amplitude and depends only upon thermal excitations. Those conditions obtain only at low power levels. At higher powers transitions to the upper state occur at a faster rate than decays to the lower state, effectively saturating the two level system and leading to increased mean free paths.

There is, however, a competing relaxation mechanism.[11] The sound wave compresses part of the solid and expands other parts. The two level systems attempt to maintain thermal equilibrium with their surroundings by exchanging energy irreversibly with the sound wave. This process does not saturate and in the low temperature limit the inverse mean free path is proportional to T^3 and independent of frequency. This explains the curves in Fig. 6.

The same authors have measured the variation in longitudinally and traversely polarized sound velocity[5] as a function of frequency and tem-

perature using powers of 10^{-3} W/cm^2. Their results for $\Delta v/v \times 10^4$ are shown in Fig. 7. Also shown is the behavior of a quartz crystal in which $\Delta v/v = 0$. Using the Kramers-Kronig relation the variation of the sound velocity can be related to the sound absorption α:

$$\left(\frac{\Delta v}{v}\right)_\nu = P \int_0^\infty d\omega' \, \frac{c}{\pi} \, \frac{\alpha(\omega' T) - \alpha(\omega' T_0)}{\omega^2 - \omega'^2} , \tag{13}$$

and

$$\alpha_\nu(\omega T) = \pi \, \frac{n_0 M_\nu^2}{\rho v_\nu^3} \, \omega \tanh \frac{\hbar\omega}{2kT} . \tag{14}$$

Therefore

$$\left(\frac{\Delta v}{v}\right)_\nu = \frac{n_0 M_\nu^2}{\rho v_\nu^2} \, \ell n \, \frac{T}{T_0} , \tag{15}$$

where T_0 is a reference temperature. The decreasing part of the $\Delta v/v$ curve can be obtained from the relaxation described above. The quantity $n_0 M_\nu^2$ is the coupling between the sound wave and the two level systems $n_0 M_\ell^2 \sim 2.6 \times 10^8$ erg cm^{-3} and $n_0 M_t^2 \sim 1.2 \times 10^8$ erg cm^{-3} for borosilicate glass. From specific heat experiments $n_0 = 8 \times 10^{32}$ erg^{-1} cm^3, therefore $M_\ell \sim .35$ eV and $M_t = .24$ eV. That is longitudinal and transverse phonons couple equally well to the two level systems. Results for silica are very similar. This large value of the deformation potential also means a large Gruneisen parameter.

The change in velocity of light in silica and borosilicate glasses was determined[6] through measurement of the temperature dependence of the dielectric constant by monitoring the shift in resonance frequency of a microwave cavity partially filled with the sample. The results are similar to the above with a bigger difference between borosilicate and SiO_2 glasses as shown on Fig. 8. The relevant parameter is $n_0 p^2$ - where p is the dipole moment. Using n_0 from specific heat experiments, p is about 0.3 D for

SiO_2 and 0.66 D for borosilicate glass assuming the same value for n_0. It appears that different units are responsible for the motion in each of these materials. Since a Debye unit is 10^{-18} esu cm, 0.3 D corresponds to one electronic charge moving 0.06 A. Thus the low value of the dipole moment precludes the motion of single atoms for which p would be higher.

THERMAL CONDUCTIVITY

In general the thermal conductivity can be expressed in the kinetic form by

$$K = \frac{1}{3} \int c(\omega) v(\omega) \ell(\omega) d\omega \ , \qquad (16)$$

where $c(\omega)$ is the specific per unit frequency range for those modes which have a group velocity $v(\omega)$. Those which have a zero group velocity become scattering mechanisms which decrease $\ell(\omega)$. The two level systems have no group velocity thus we use the Debye expression for $c(\omega)$ and the mean free path as calculated from ultrasonic measurements.[19] At the low temperatures we only need the resonant scattering. In this case

$$\Lambda = \frac{\rho k^3 T^2}{6\pi^3 \hbar^2} \left(\frac{v_\ell}{n_0 M_\ell^2} + 2 \frac{v_t}{n M_t^2} \right) \int_0^\infty \frac{x^3 e^x (e^x+1)}{(e^x-1)^3} \, dx \ . \qquad (17)$$

All the quantities are known and the integral is just a number. At 0.2, $\lambda = 1.1 \times 10^5$ W/cm K and Zaitlen and Anderson[19] find 9×10^{-6} W/cm K for borosilicate glass. They also find that they can reproduce the entire thermal conductivity curve including the plateau at 10 K if they use the non-resonant scattering and let $n(\varepsilon) = n_0 + n_2' \varepsilon^2$ as required by the specific heat measurements. Their results for SiO_2 and borosilicate glass are quite good. For the polymer polymethyl methacrylate (PMMA) and for GeO_2 their results are not as encouraging.

Thus all these experiments, the specific heat, ultrasonic attenuation, sound velocity, dielectric constant and thermal conductivity appear to be explained by a uniform distribution of two level systems.

THERMAL EXPANSION

The original models for these systems ascribed the two levels to phonon assisted tunneling between two configurations of groups of atoms having about the same energy.[11] The energy separation of the two levels was $E = \sqrt{\Delta^2 + \Delta_o^2}$ where Δ_o is the tunnel splitting for the symmetric case

$$\Delta_o = \hbar\Omega \sqrt{\sigma/\pi}\, e^{-\sigma} \tag{18}$$

where $\sigma \propto \sqrt{V}\, d$ and $\hbar\Omega \sim 10^{-2}$ eV and E is the energy difference between the ground states of the two wells. These quantities are defined in the inset of Fig. 9. Up to now we have not needed any property of the tunneling to explain the results.

Recently White[7] has measured the linear thermal expansion α of SiO_2 down to 1.5 K and finds that $-\alpha/T^3$ increases dramatically at the lowest temperatures as shown in Fig. 9. Similar preliminary measurements have been performed on PMMA and in that case $+\alpha/T^3$ increases at low temperature.[20] The thermal expansion is related to the specific heat by $\alpha = \gamma c\rho/3B$ where B is the bulk modulus, ρ is the density and γ the Gruneisen parameter. γ is defined by

$$\gamma = -\frac{\partial \ln \omega}{\partial \ln V} \tag{19}$$

For SiO_2, γ is about -40 and for PMMA, γ is about +40 where $c = c_1 T$ only.

One can explain the large positive Gruneisen parameters for PMMA by noticing that as the temperature decreases the wells come closer together.

Thus both V and d decrease slightly, but the tunneling frequency increases steeply because V and d appear in the exponent. The same explanation suffices for SiO_2 because when the temperature is lowered the SiO_2 lattice expands. Thus the wells get further apart and the tunneling frequency decreases and α/T^3 becomes more negative. Similar large expansion coefficients were found for OH^- doped NaCl in which it is known that the OH tunneled between equivalent potential minima in the Cl^- vacancy.[21] However, in our case a two level system would suffice if the level spacing somehow depended upon the distance between wells.

FAR-INFRARED STUDIES

For several years, Sievers and his students have looked for evidence of the low energy states in far infrared absorption. Recently, Mon and Chabal succeeded in measuring the optical absorption in four amorphous materials, GeO_2, PMMA and two pieces of SiO_2 containing different amounts of water.[9] The data obtained at 4.2 K are shown in Fig. 10. At first sight, the spectra show little similarity, and are strongly sample dependent, as evidenced in curves C and D for SiO_2. It turns out, however, that all spectra have a very characteristic temperature dependence in common, which is shown in Fig. 11. Mon and Chabal measured the absorption between 1.2 and 4.2 K, for PMMA even between 0.54 K and 10 K. In their paper[9], Mon et al. show that a straightforward description of this temperature and frequency dependence can be achieved with a level diagram as shown in Fig. 12b. Each absorbing center consists of three states, two of which are closely spaced ($r\hbar\omega$, $r \sim 0.05$) relative to the spacing of the third state ($\hbar\omega$). The optical absorption is assumed to take place

only between the states labelled 1 and 2. The temperature and frequency dependence results from the thermal population of the three states. At low frequencies ($< 6\ cm^{-1}$), an increase in temperature causes a decrease in absorption, since state 2 becomes increasingly more populated, while at higher frequencies, state 2 remains thermally depopulated. The increase in absorption in this frequency range results from a thermal population of state 1, out of which the absorption takes place.

The optical absorption and the model used to describe it shows a great deal of resemblance with that of alkali halide crystals doped with certain impurities known to tunnel between certain equivalent potential wells within the lattice site they occupy.[3] There the closely spaced states result from tunneling, while the wide spacing is caused by oscillator states. A spectroscopic study of the temperature dependence of absorption in several tunnel systems, e.g., KCl: Li, NaCl:OH, has been made by Kirby et al.[22] Guided by this similarity, Mon et al. argue that their observations in the amorphous materials result from similar tunneling and oscillator states, except that in the amorphous materials the splittings $\hbar\omega$ (and $r\hbar\omega$) are spread over a wide frequency range, possibly with a constant density of states $n(\varepsilon)$ equal to that derived from the linear specific heat anomaly discussed earlier.

Since the oscillator strength of the far infrared transition $\hbar\omega$ is not known, and since it may also be frequency dependent, the optical data cannot be used for an independent determination of the density of states $n(\varepsilon)$. In amorphous substances $n(\varepsilon)$ is therefore usually determined from specific heat measurements. Figure 4 shows an analysis by Stephens of

the low temperature specific heat of amorphous SiO_2.[1] In the tunneling model[11] proposed to explain the low energy states in glasses, it is postulated that the states observed in specific heat are also responsible for the phonon scattering. This we want to explore in some detail in the following.

THERMAL CONDUCTIVITY IN AN ELECTRIC FIELD

In an applied electric field E, tunneling defects in crystalline solids become polarized[3], and hence, their energy splitting will change. Resonant scattering of phonons by these states will, consequently, move to a different frequency.[3] Stephens looked for a similar effect in glasses.[2,3] We have seen above that the thermal conductivity measurement, as well as the temperature and frequency dependence of the speed of sound and the real part of the dielectric constant (i.e., the speed of electromagnetic waves in the medium) can be interpreted with the assumption of a constant density of states of the tunneling defects. The density of states derived from specific heat measurements, however, shows a nonlinear contribution (approximately proportional to ε^2) in the frequency range of interest for heat conduction below 1 K, See Fig. 4. Hence, Stephens argued as follows: If the density of states of tunneling defects is indeed constant, then an electric field will not alter the density of states $n(\varepsilon,E)$ at a certain energy ε, since the number of states removed by the field E will equal that of the states whose frequency will be changed to ε by the field. Hence, regardless of the magnitude of the dipole moment of the tunneling defects, the thermal conductivity $\Lambda(T,E)$ should be field independent. Stephens measured $\Lambda(T,E)$ of a thin plate of silica with and

without an applied field of 10^5 volt/cm, see Fig. 13 and 14. He analyzed the null effect observed in two ways: Using the dipole moment determined by Schickfus et al.[6], he concluded that the density of the phonon scattering states had to be constant to within 6% over the range of frequencies carrying the bulk of the heat in the temperature range of his measurement (0.16 to 1.1 K, corresponding to the range of frequencies $\nu = \omega/2\pi = 10^{10}$ to 7×10^{10} sec^{-1}). In this range, the density of states obtained from specific heat (see Fig. 4) actually varies by a factor of two. Alternatively, Stephens could derive an upper limit for the dipole moment assuming that the density of the states which cause the phonon scattering was actually given by $n(\varepsilon)$ determined from the specific heat. In that case, the density of states should vary with the applied field, and hence the absence of an effect of E on Λ could be used to determine an upper limit of the dipole moment of the tunneling states. Under this assumption, Stephens found an upper limit of the dipole moment in SiO_2 of 0.1 D = 0.02 eA (local field corrected), smaller than the value determined by Schickfus et al.[6] by a factor of three, and unreasonably small for tunneling atoms or even silicon oxide molecules.

DENSITY OF STATES FROM SPECIFIC HEAT MEASUREMENTS

The question whether the specific heat density of states $n(\varepsilon)$ is equal to that responsible for the phonon scattering, as postulated in the tunneling model, was also studied by Goubau and Tait.[24] Since the tunneling frequency, and hence the coupling to the lattice should depend greatly on the barrier height, one of the first predictions of the tunneling model of glasses[11] was that the observed specific heat should

be dependent on the time during which the measurement was performed. For short times, only the strongly coupled tunneling states can take up energy from the lattice; and hence the specific heat should appear smaller. Goubau and Tait were unable to detect such an effect even when the sample dimensions were chosen such that the heat could propagate through the sample in times of the order of 10^{-5} sec. Figure 15 shows the data obtained on polymethyl methacrylate. Although the tunneling model can probably be modified in such a way as to be brought into agreement with this result, the explanation of the discrepancy is probably much simpler, as will be discussed next.

In the earlier studies of the specific heat anomaly of amorphous dielectrics, no evidence was found that it was sample dependent. Hence, the theoretical model was designed with the assumption that the anomaly (as well as the thermal conductivity) is independent of the particular sample. A systematic study by Stephens, however, has turned up evidence that this conclusion was premature, at least as far as the specific heat anomaly is concerned.[25] Figure 16 shows the specific heat of amorphous As_2S_3. With increasing sample purity and/or perfection, a Schottky type anomaly disappears in As_2S_3, as does an anomaly beginning below 0.1 K, leaving an anomaly of the usual form (closed circles). Further care in producing the sample (chemical purity and/or physical perfection?), however, makes this anomaly shrink by more than a factor of two (open circles). The thermal conductivity of the latter two samples, however, differs by less than 20% (and even this difference is believed to be the result of the poor definition of the geometry of the sample[25]). Similar results

were found for B_2O_3 [2,8,26] and the ionic glass $CaK(NO_3)_3$ [25]. In these glasses, a reduction of the anomalous specific heat resulted in zero change of the thermal conductivity. Consequently, the entire removable portion of the specific heat anomaly apparently does not scatter phonons. Whether all or at least part of the excitations causing the excess specific heat in the sample with the lowest specific heat scatter phonons, has to be left as an open question. Recently, the specific heat of amorphous solids was measured for the first time to temperatures well below 0.1 K.[2] The results obtained on several samples of SiO_2 are shown in Fig. 17. In addition to the sample dependence, the low temperature data also show the limits to what is called the "linear specific heat anomaly", as inferred from the data obtained above 0.1 K (Fig. 17, see the data by Zeller and Pohl). It is important to realize, though, that the thermal conductivity of SiO_2 was found to be entirely sample independent[2].

We are thus lead to the conclusion that at best only a fraction of the states seen in specific heat measurements are caused by the postulated tunneling states, and hence the specific heat results, which played such a major role in the formulation of the tunneling model,[11] have to be viewed with caution. On the other hand, we have at present no reason to believe that the thermal conductivity of amorphous solids is not truly intrinsic. It is most easily explained with the assumption of a highly constant density of states of scattering centers.(See the work on $\Lambda(T,E)$[23], and both the ultrasonic and the dielectric work by the Grenoble group[4-6] lends strong support to the picture of a constant density of highly anharmonic states of low energy in all amorphous solids.) Finally, the

far infrared absorption measurements in Sievers' group[9] provide probably the most direct resemblance between these states and the tunneling-oscillator states studied extensively in crystalline solids containing certain defects. This raises the interesting question whether an "amorphous" thermal conductivity, and/or a linear specific heat anomaly can also exist in sufficiently disordered crystalline solids. Figure 18 shows the discovery of phonon scattering by tunneling defects in an alkalide halide host crystal, NaCl, by Klein.[27] The thermal conductivity decreases with increasing impurity concentration (identified since as the tunneling OH^- - ion.[28]) The phonon scattering was explained by Sussman[18] as resulting from resonance scattering by tunneling defects. Sussman argued that the conductivity varied roughly as T^2 in the highly doped crystal, from which he concluded that the density of states $n(\varepsilon)$ had to be constant, in a manner identical to that postulated later in glasses.[11] The specific heat of NaCl:OH has actually never been measured. In subsequent studies of more carefully doped NaCl:OH crystals it has been found, however, that $\Lambda(T)$ shows a far more pronounced structure than shown in Fig. 18. From these findings it followed that the density of states of the tunneling defects in this material is really not very constant. Rather, all the OH^- - ions in NaCl have fairly equal level schemes, similar to those of the other well known tunneling defects[3], e.g. KCl:CN or KCl:Li.

A linear specific heat anomaly in doped alkali halides has actually been observed in NaBr:F,[29] see Fig. 19. Rollefson explained this with the tunneling theory developed by Sussman, assuming a spread of asymmetric

wells between which the F^- - ion could tunnel. Rollefson found, however, that the thermal conductivity was not affected by these tunneling defects, indicating that their coupling to the lattice had to be much weaker than, for instance, that of OH^- in NaCl. Rollefson did observe that the anomalous specific heat varied linearly with the fluorine ion concentration in the crystal.

So much for the doped alkali halide crystals. These examples show that a behavior similar to that common to all amorphous solids can be found in crystals under certain conditions. Another interesting example for glass-like behavior has been discovered by Bilir[30] and by Slack et al.[31] in crystalline YB_{66}. The low temperature thermal conductivity is almost exactly identical to that of silica, and the specific heat shows a linear anomaly at low temperatures of 2.6×10^{-6} J gm^{-1} K^{-2} which is similar to the value of 1.1×10^{-6} J gm^{-1} K^{-2} for SiO_2. Bilir has suggested that these phenomena are connected with low energy tunneling states of the yttrium ion between almost equivalent potential wells.

Clearly, more work is needed in order to demonstrate under what conditions glass-like thermal behavior can be observed in disordered crystals, and, at Cornell, work is going on in this direction.

In conclusion, we want to re-emphasize the point which we find most remarkable about the glassy anomalies: Why do all amorphous solids appear to have the same low temperature thermal conductivity, both in temperature dependence and absolute magnitude? We believe that the understanding of this phenomenon will be crucial for the understanding of the origin of this anomaly.

References

*This work has been supported in part by the Energy Research and Development Administration under contract No. E(11-1) 3151, Technical Report No. (C00-3151-61) and in part by the National Aeronautics and Space Administration, Grant No. NGL 33-018-003.

1. Stephens, R. B. 1973. Phys. Rev. B8: 2896-2905.
2. Lasjaunias, J. C., A. Ravex and M. Vandorpe. 1975. Solid State Comm. 17: 1045-1049.
3. Narayanamurti, V., R. O. Pohl. 1970. Rev. Mod. Phys. 42: 201-236.
4. Arnold, W., S. Hunklinger, S. Stein and K. Dransfeld. 1974. J. Non-Cryst. Solids 14: 192-200, and references cited therein.
5. Piché, L., R. Maynard, S. Hunklinger and J. Jäckle. 1974. Phys. Rev. Letts. 32: 1426-1429. The change in velocity of transverse modes was reported by Hunklinger, S. and L. Piché. 1975. Solid State Comm. 17: 1189-1192.
6. von Schickfus, M., S. Hunklinger, and L. Piché. 1975. Phys. Rev. Letts. 35: 876-878.
7. White, G. K. 1975. Phys. Rev. Letts. 34: 204-205.
8. Szeftel, J. and H. Alloul. 1975. Phys. Rev. Letts. 34: 657-660.
9. Mon, K. K., Y. J. Chabal, and A. J. Sievers. 1975. Phys. Rev. Letts. 35: 1352-1355.
10. Morgan, G. J. and D. Smith. 1974. J. Phys. C7: 649-664. Walton, D. 1974. Solid State Comm. 14: 335-339. See also the review by Böttger, H. 1974. Phys. Stat. Sol. (b) 62: 9-42.

11. Anderson, P. W., B. I. Halperin and C. M. Varma. 1972. Phil. Mag. 25: 1-9.

Jäckle, J. 1972. Z. Physik 257: 212-223.

Phillips, W. A. 1972. J. Low Temp. Phys. 7: 351-360.

12. See, for example, the solid state text book by Kittel, C. 1971. Introduction to Solid State Physics. 4th edit. John Wiley and Sons, Inc., New York, N. Y., pg. 215.

13. Anderson, O. L. 1959. J. Phys. Chem. Solids. 12: 41-52.

14. Zeller, R. C. and R. O. Pohl. 1971. Phys. Rev. B4: 2029-2041.

15. Flubacher, P., A. J. Leadbetter, J. A. Morrison, and B. D. Stoicheff. 1959. J. Phys. Chem. Solids 12: 53-65.

Hornung, E. W., R. A. Fisher, G. E. Brodale and W. F. Giauque. 1969. J. Chem. Phys. 50: 4878-4886.

16. N. Bilir and W. A. Phillips. 1975. Phil. Mag. 32: 113-122.

17. Leadbetter, A. J. 1969. J. Chem. Phys. 51: 779-786.

18. Sussman, J. A. 1964. Phys. Kondens Materie 2: 146-160.

19. Zaitlin, M. P. and A. C. Anderson. 1975. Phys. Stat. Sol. (b) 71: 323-327.

20. Lyon, K. and G. L. Salinger, unpublished.

21. Case III, C. R. and C. A. Swenson. 1974. Phys. Rev. B9: 4506-4511.

22. Kirby, R. D., A. E. Hughes and A. J. Sievers. 1970. Phys. Rev. B2: 481-509.

23. Stephens, R. B. 1976. submitted to Phys. Rev. B.

24. Goubau, W. M. and R. H. Tait. 1975. Phys. Rev. Lett. 34: 1220-1223.

25. Stephens, R. B. 1975. accepted for publication in Phys. Rev. B.

26. Lasjaunias, J. C., D. Thoulouze and F. Pernod. 1974. Solid State Comm. 14, 957-961.

27. Klein, M. V. 1961. Phys. Rev. 122, 1393-1402.

28. Rosenbaum, R. L., C. K. Chau and M. V. Klein. 1969. Phys. Rev. 186: 852-864.

29. Rollefson, R. J. 1972. Phys. Rev. B5: 3235-3253.

30. N. Bilir, "Low Temperature Heat Capacities of Open-Structured Crystals", Ph.D. Thesis, Stanford University, Dept. of Materials Science and Engineering, May 1974, unpublished.

31. Slack, G. A., D. W. Oliver and F. H. Horn. 1971. Phys. Rev. B4: 1714-1720, Also Slack, G. A., D. W. Oliver, G. D. Bower and J. D. Young, J. Phys. Chem. Solids, to be published.

Figure Captions

1. Specific heat of non-crystalline solids below 1 K plotted as c/T vs T . After Stephens, Ref. 1.
2. Thermal conductivity of non-crystalline solids. After Stephens, Ref. 1. Note the extension of the SiO_2 data[2] to 0.025 K.
3. Specific heat of crystalline and vitreous SiO_2 plotted as c/T^3 vs T to show deviation from the Debye T^3 law. The line marked quartz was measured by Zeller and Pohl[14] and the dashed line represents the value of c/T^3 calculated from elastic measurements. The dashed line $c_{3,D}$ is the Debye contribution to the specific heat of vitreous silica calculated through Eq. 7 (Ref. 14). The curves represent specific heat measurements on different samples of vitreous silica, Stephens[1], Zeller[14], Flubacher[15], Hornung[15].
4. Density of states for SiO_2 glass. The experimental density of states, derived from specific heat measurements, was calculated under the assumption that the excess states are harmonic oscillators, as are phonons. If the systems consisted of two levels, their density of states would be twice as large. Systems with energy level spacing Δ are frozen out at $\Delta/kT = 1/3$, so, for instance, all the states up to $\Delta/k = 1$ K are involved in the specific heat at 1/3 K. The top scale on this figure shows the temperature at which a system with energy level spacing Δ becomes thermally excited. After Stephens, Ref. 1.
5. Ultrasonic attenuation of borosilicate and SiO_2 glass as a function of acoustic intensity. The inverse mean free path is that due to

the two level system only. At power levels below 10^{-7} W/cm^2 the inverse mean free path is constant and for the borosilicate glass glass varies as ω; i.e., $(940/732)^2 = 1.67 = 1/0.6$. At powers above 10^{-7} W/cm^2 the attenuation is proportional to the power to the 0.5 power in agreement with theory.[4] After Arnold et al., ref. 4.

6. Temperature dependence of the ultrasonic attenuation of borosilicate glass at 940 MHz at two different powers (Arnold et al., ref. 4). The full circles show the attenuation in the almost unsaturated region and the increase in this attenuation below 0.6 K is clearly seen. The triangles show the saturated attenuation approaching a constant value of 0.6 dB/cm^2. Curve 3 was obtained by subtracting curve 2 from curve 1. Curve 4 was obtained by subtracting 0.6 dB/cm^2 from curve 2. The T^3 dependence of curve 4 is due to relaxation of the two level systems as described in the text.

7. Relative variation of the longitudinal sound velocity $\Delta v_\ell / v_\ell$ plotted as a function of the temperature on a logarithmic scale. The straight line represents a variation proportional to ℓn T. The solid lines represent the theoretical prediction for the sum of the contribution of the resonant and the relaxation process, the latter dominating above 0.6 K. The dash-dot line represents the contribution of the resonant interaction alone assuming $n(\varepsilon) = n_o + n_2'\varepsilon^2$. The filled triangles show the variation for crystalline silica. After Piché et al., ref. 5.

8. Relative variation of the velocity of light $\Delta c/c$ at 1.1 GHz in borosilicate and SiO_2 glass plotted versus temperature. The proportionality

constant relating $\Delta c/c$ to $\ell n\ T/T_o$ is different for the two materials leading to different dipole moments. von Schickfus et al., ref. 6.

9. The thermal expansion α of vitreous silica plotted as α/T^3 versus T. After White, ref. 7. Note that the thermal expansion of SiO_2 is negative over the entire region. The increase in the magnitude of α/T^3 may be due to phonon assisted tunneling the model for which is shown in the inset. A particle or group of particles may be in two states separated by a distance d and a barrier height V. The energy of the system in the two states differ by a small amount ε. At low temperatures the particles can get from one state to the other by tunneling through the barrier with the energy made up by the phonons.[11]

10. Absorption coefficient versus frequency for four different glasses at 4.2 K. Mon et al., ref. 9.

11. Changes in absorption coefficient with temperature versus frequency. The dots represent the experimental data, the dashed line the two-level model, and the solid line the three-level model. Mon et al., Ref. 9.

    (a) PMMA: $\alpha(4.2\ K) - \alpha(1.2\ K)$. Parameters for the three-level model are $g_o = 3.6 \times 10^{-2}$, $r = 1/20$.

    (b) PMMA: $\alpha(0.97\ K) - \alpha(0.55\ K)$

    (c) PMMA: $\alpha(8.68\ K) - \alpha(4.25\ K)$

    (d) SiO_2(with 600 ppm H_2O): $\alpha(4.2\ K) - \alpha(1.2\ K)$. Parameters for the three-level model are $g_o = 3.8 \times 10^{-3}$, $r = 1/40$.

(e) SiO_2 (water free) $\alpha(4.2\ K) - \alpha(1.2\ K)$. Parameters for the three-level model are $g_o = 3.8 \times 10^{-3}$, $r = 1/40$.

(f) GeO_2: $\alpha(4.2\ K) - \alpha(1.2\ K)$. Parameters for the three level model are $g_o = 2 \times 10^{-1}$, $r = 1/20$.

12. Two models of far infrared absorption by the low energy states (a) Two level, (b) Three-level. The far infrared transition is labeled $\hbar\omega$. Mon et al., ref. 9.

13. Thermal conductivity of the vitreosil high electric field sample in zero field. The vertical scale was determined by comparison to previous thermal conductivity measurements on the same material (solid line). The deviation below 0.2 K is due to the thermal resistance of an indium-glass interface, which was included in the measurement since the cold thermometer was soldered to the heat sink rather than separately to the glass. Stephens, Ref. 23.

14. Thermal conductivity of the vitreosil high electric field sample plotted as the percentage deviation from a polynomial fit. The filled circles are the data for $E = 0$, the open circles are the data for $E = 10^5$ V/cm. Stephens, Ref. 23.

15. The specific heat of polymethyl methacrylate as measured on both long (5 sec) and short (50 μsec) time scales. The closed circles are short-time data determined from the thermal diffusivity α. The open circles are short-time data determined from the maximum amplitude, ΔT_m, of the heat-pulse signal at the bolometer. The dashed line is the tunneling-model prediction.[11] The solid line

is the long-time data for PMMA from Stephens, R. B., G. S. Cieloszyk, & G. L. Salinger. 1972. Phys. Letts. 38A: 215-217.

16. Specific heat of four As_2S_3 samples plotted as c/T vs T^2. The line marked C_{Deb} is the heat capacity predicted by the Debye model. The two upper curves are from samples which were produced at Cornell with successively more care to remove water of hydration. The next curve is from a sample which was supplied by A. J. Leadbetter. The lowest set of data is from a sample which was made by F. J. DiSalvo at Bell Labs. If one assumes that the differences between the upper three and lowest sets of data are due to the presence of two-level systems, one can calculate the density of these systems to be 68 x 10^{16} cm^{-3} for the upper curve, 26 x 10^{16} for the second one, and $\sim 10^{16}$ cm^{-3} for the third. Spark source mass spec analysis of the four measured samples showed the following impurity concentrations in the order given above: 1) 10^{19} to 10^{20} cm^{-3} Sb and 10^{17} to 10^{18} cm^{-3} Rb; 2) 10^{17} to 10^{18} cm^{-3} and 10^{16} to 10^{17} cm^{-3} Cd; 3) 10^{17} to 10^{18} cm^{-3} Ge; 4) nothing detectable; After Stephens, .. Ref. 25.

17. Specific heat of vitreous SiO_2 above 0.025 K, Suprasil and Spectrosil B have large OH concentrations, but small metal ion concentrations. Suprasil has 130 ppm chlorine and 100 ppm fluorine. Suprasil W has low OH and metal ion concentrations, but 230 ppm chlorine and 290 ppm fluorine (all numbers according to the manufacturer). Note that Spectrosil B and Suprasil have identical specific heats in the temperature range where both were measured ($T > 0.1$ K). Note also that

SiO_2 with low OH, but high ($\sim$ 50 ppm) metal ion concentrations has been found to have lower specific heats than Spectrosil B above 0.5 K; this difference, however, vanishes below that temperature (R. B. Stephens, Cornell Ph.D. Thesis, 1974, unpublished). The dashed line marks the Debye specific heat of vitreous SiO_2, $C_{Deb} = 8\ T^3$ erg $g\bar{m}^1\ K^{-4}$ based on $v_t = 3.75 \times 10^5$ cm/sec and $v_t = 5.80 \times 10^5$ cm/sec. After Lasjaunias et al., Ref. 2.

18. Thermal conductivity of commercial NaCl crystals from Harshaw and Optovac compared with a natural crystal of Baden halite and two Cornell grown crystals. The dashed line varies as T^2. After Klein, Ref. 27.

19. Specific heat of NaBr containing different amounts of NaF in solid solution. The dashed lines vary as T. After Rollefson, Ref. 29.

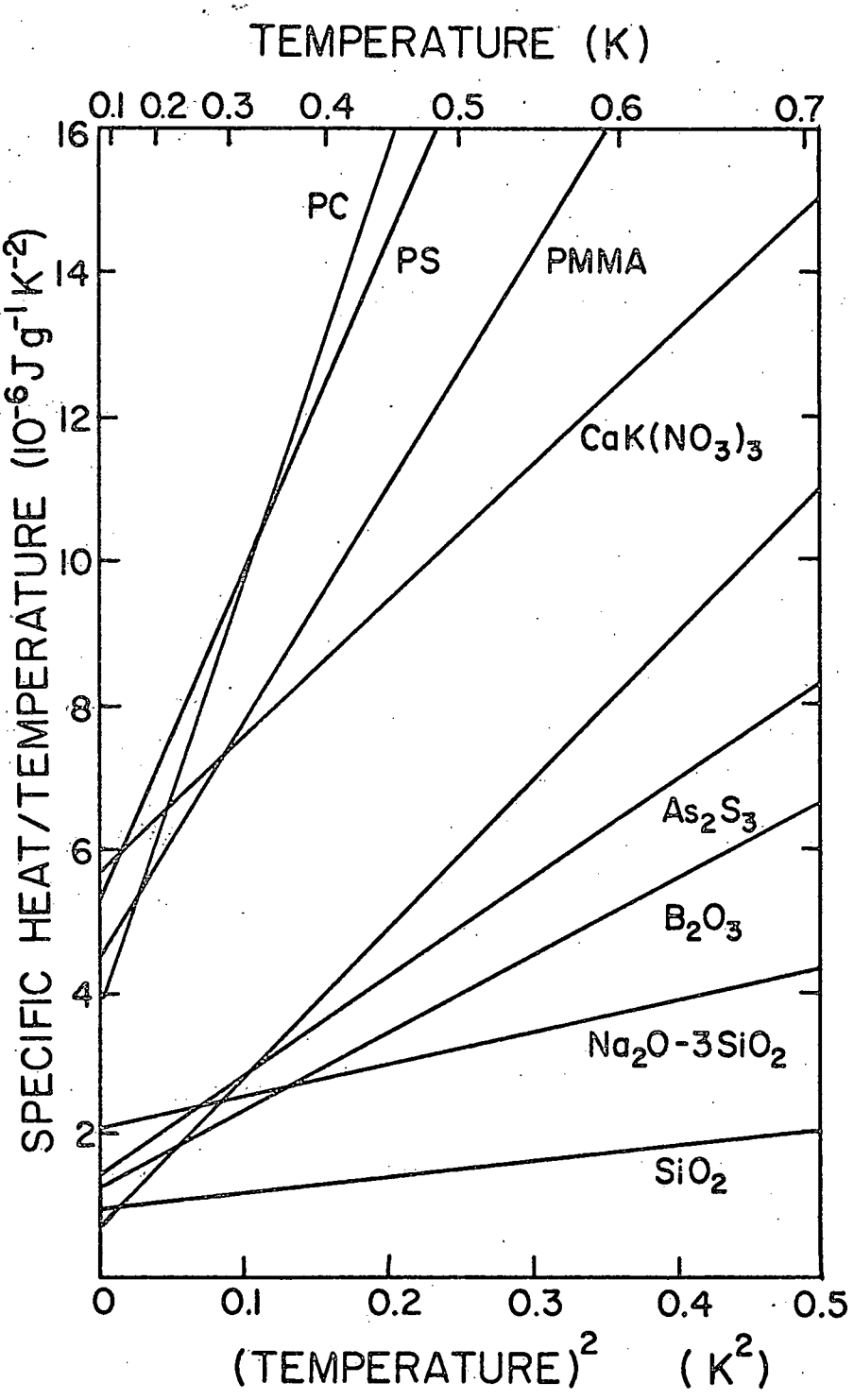
TEMPERATURE (K)
0.1 0.2 0.3 0.4 0.5 0.6 0.7
16
14
12
10
8
6
4
2
SPECIFIC HEAT/TEMPERATURE (10^{-6} J g^{-1} K^{-2})
PC
PS
PMMA
CaK(NO$_3$)$_3$
As$_2$S$_3$
B$_2$O$_3$
Na$_2$O-3SiO$_2$
SiO$_2$
0
0.1
0.2
0.3
0.4
0.5
(TEMPERATURE)^2 (K^2)

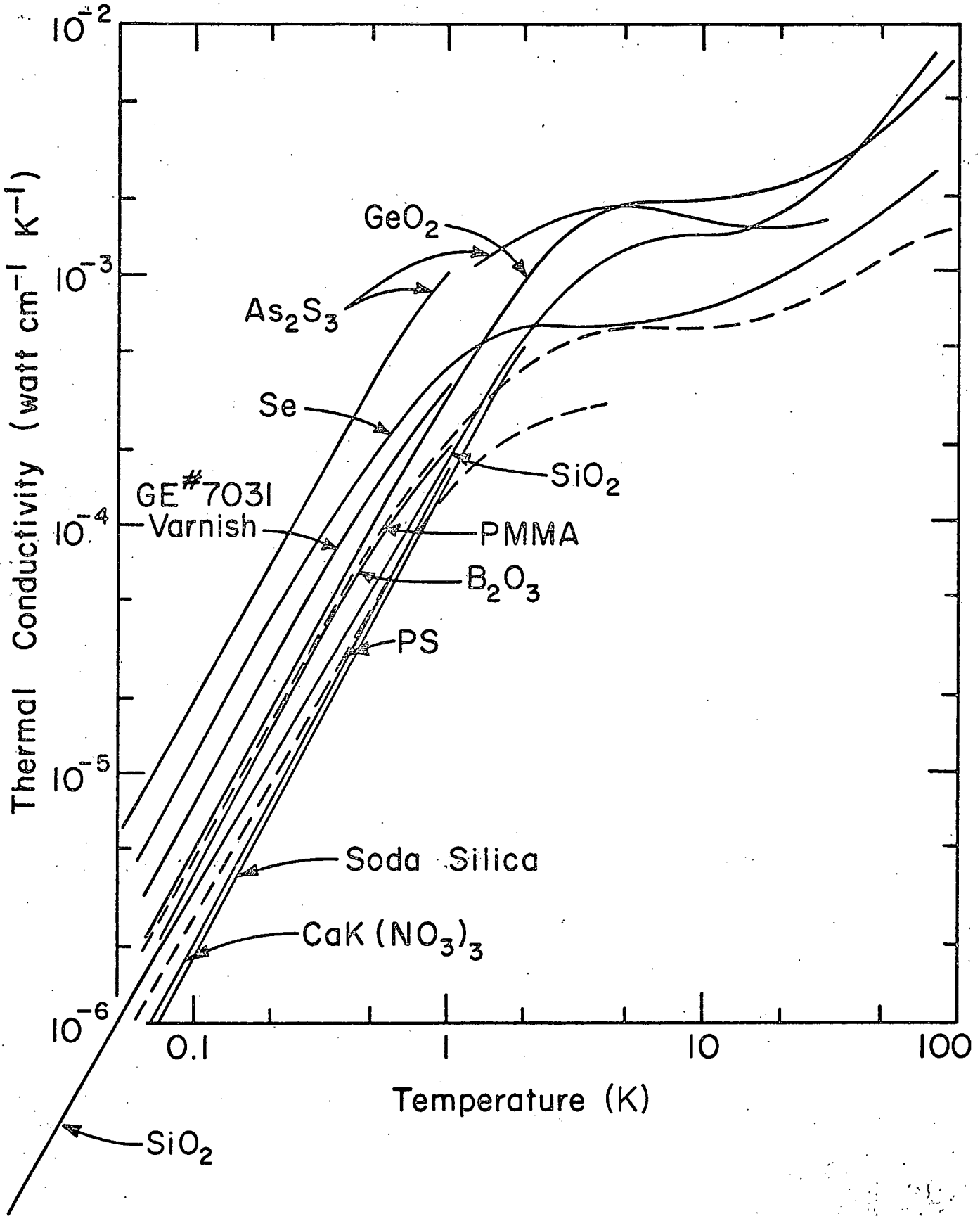
Thermal Conductivity (watt cm⁻¹ K⁻¹)
10⁻²
10⁻³
10⁻⁴
10⁻⁵
10⁻⁶
0.1
1
10
100
Temperature (K)
GeO₂
As₂S₃
Se
GE #7031 Varnish
SiO₂
PMMA
B₂O₃
PS
Soda Silica
CaK(NO₃)₃
SiO₂

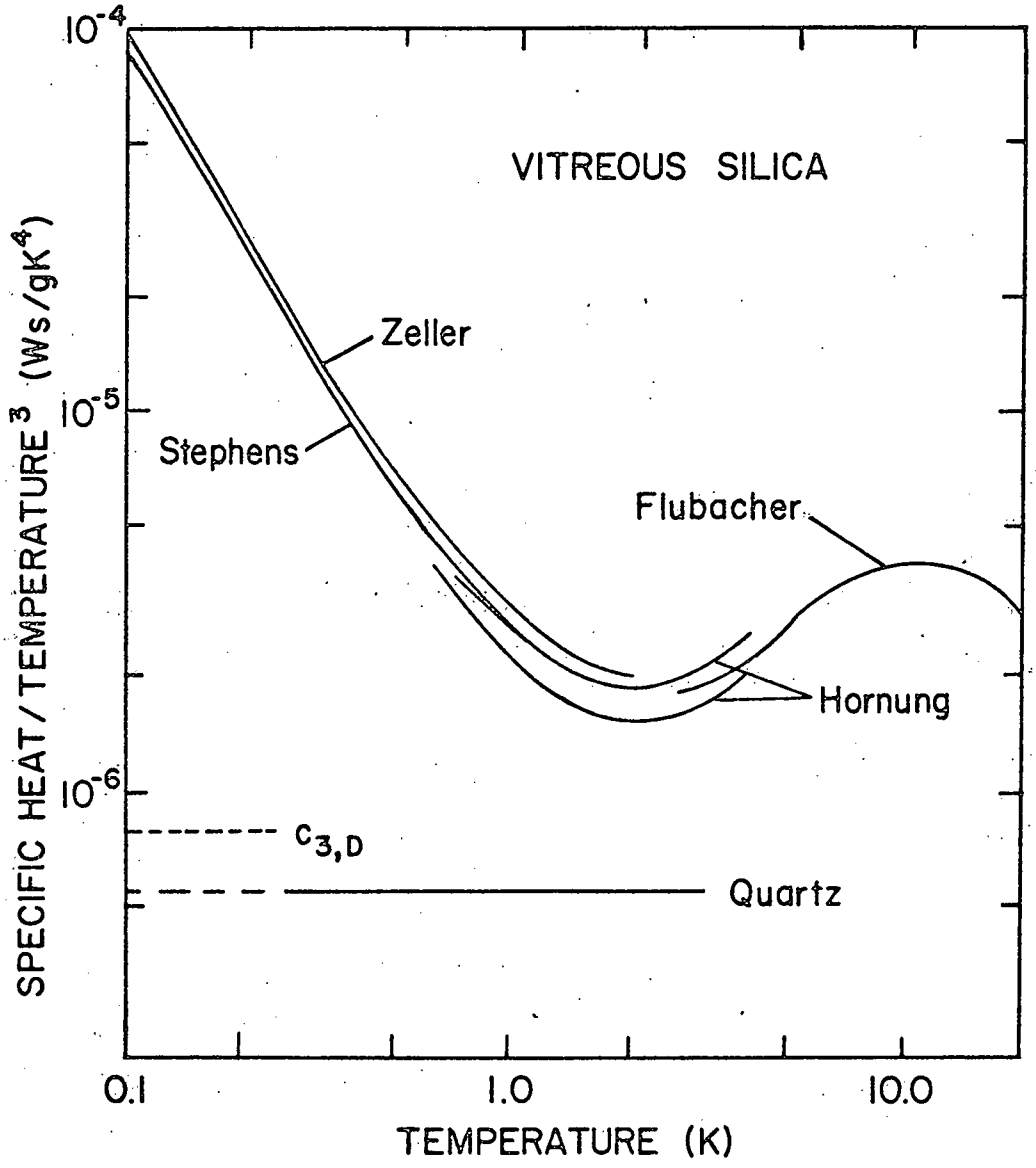
VITREOUS SILICA
Zeller
Stephens
Flubacher
Hornung
$C_{3,D}$
Quartz
10^{-4}
10^{-5}
10^{-6}
SPECIFIC HEAT / TEMPERATURE^3 (Ws/gK^4)
0.1
1.0
10.0
TEMPERATURE (K)

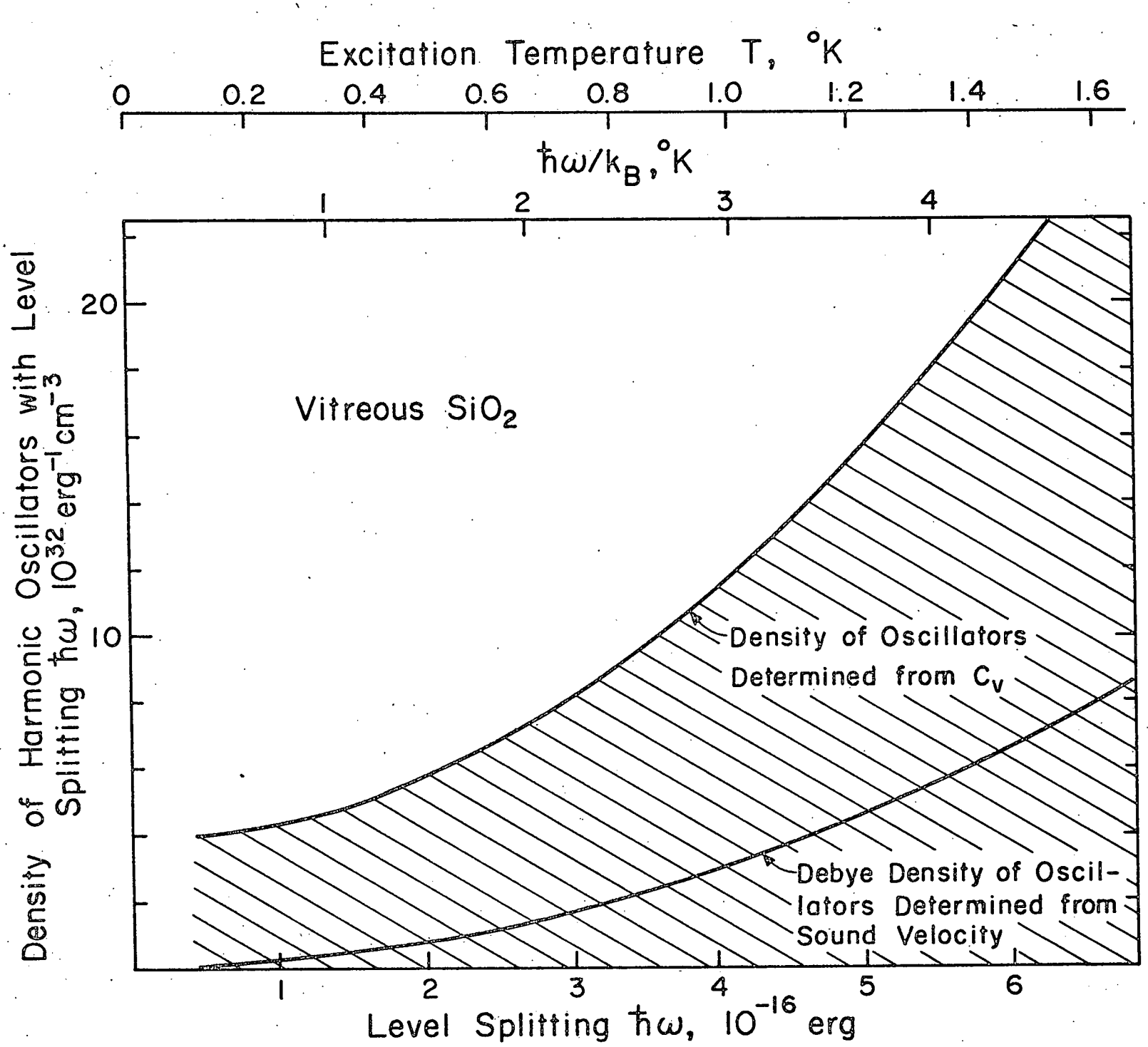
Excitation Temperature T, °K
0
0.2
0.4
0.6
0.8
1.0
1.2
1.4
1.6
ħω/k_B, °K
1
2
3
4
Density of Harmonic Oscillators with Level Splitting ħω, 10^32 erg^-1 cm^-3
20
10
Vitreous SiO2
Density of Oscillators Determined from C_v
Debye Density of Oscillators Determined from Sound Velocity
1
2
3
4
5
6
Level Splitting ħω, 10^-16 erg

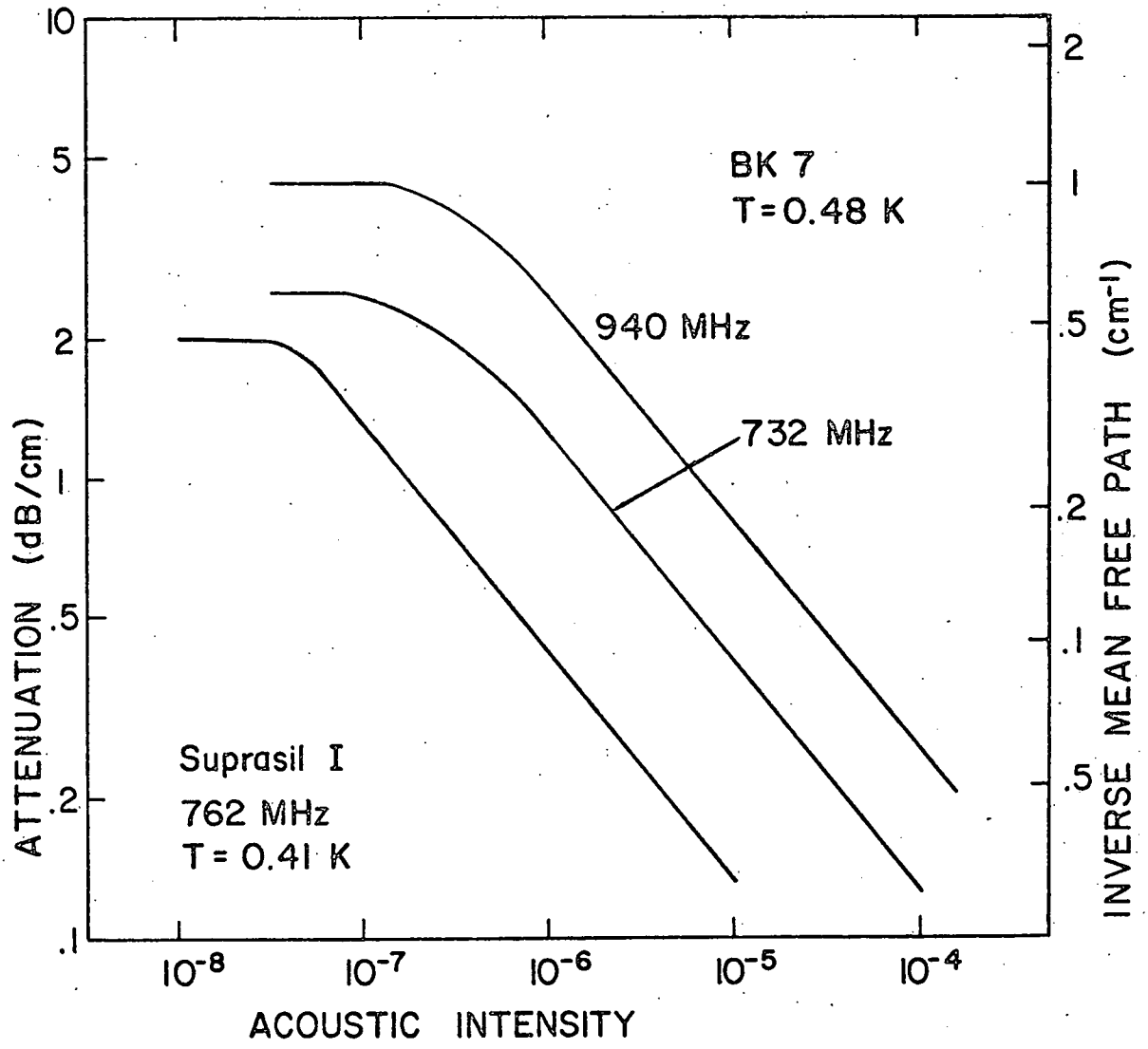
10
5
2
1
.5
.2
.1
2
1
.5
.2
.1
.5
BK 7
T=0.48 K
940 MHz
732 MHz
Suprasil I
762 MHz
T = 0.41 K
10^{-8}
10^{-7}
10^{-6}
10^{-5}
10^{-4}
ACOUSTIC INTENSITY
ATTENUATION (dB/cm)
INVERSE MEAN FREE PATH (cm^{-1})

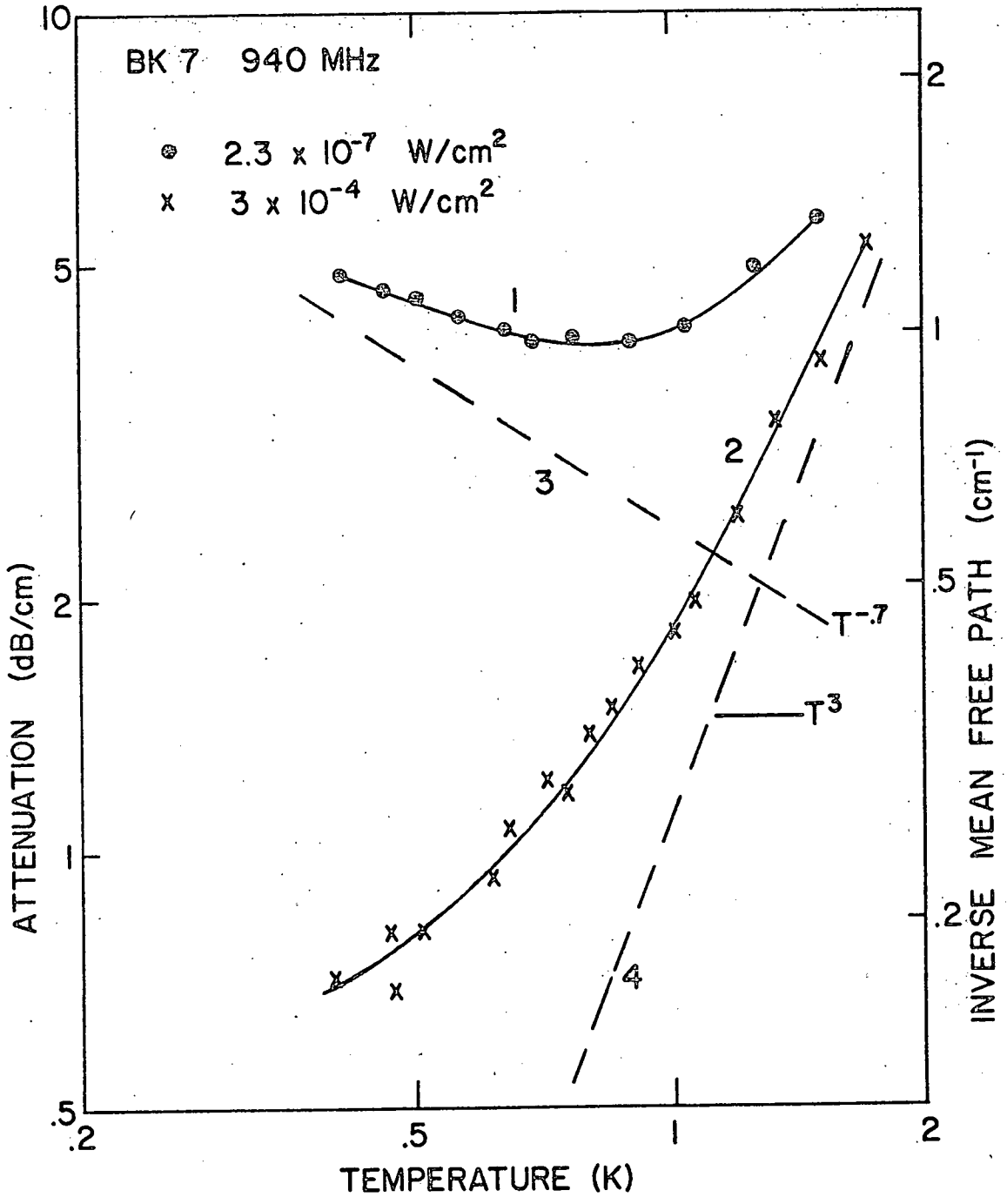
BK 7 940 MHz
2.3 x 10⁻⁷ W/cm²
3 x 10⁻⁴ W/cm²
1
2
3
4
T^-.7
T^3
ATTENUATION (dB/cm)
INVERSE MEAN FREE PATH (cm⁻¹)
TEMPERATURE (K)
10
5
2
1
.5
.2
.5
1
2

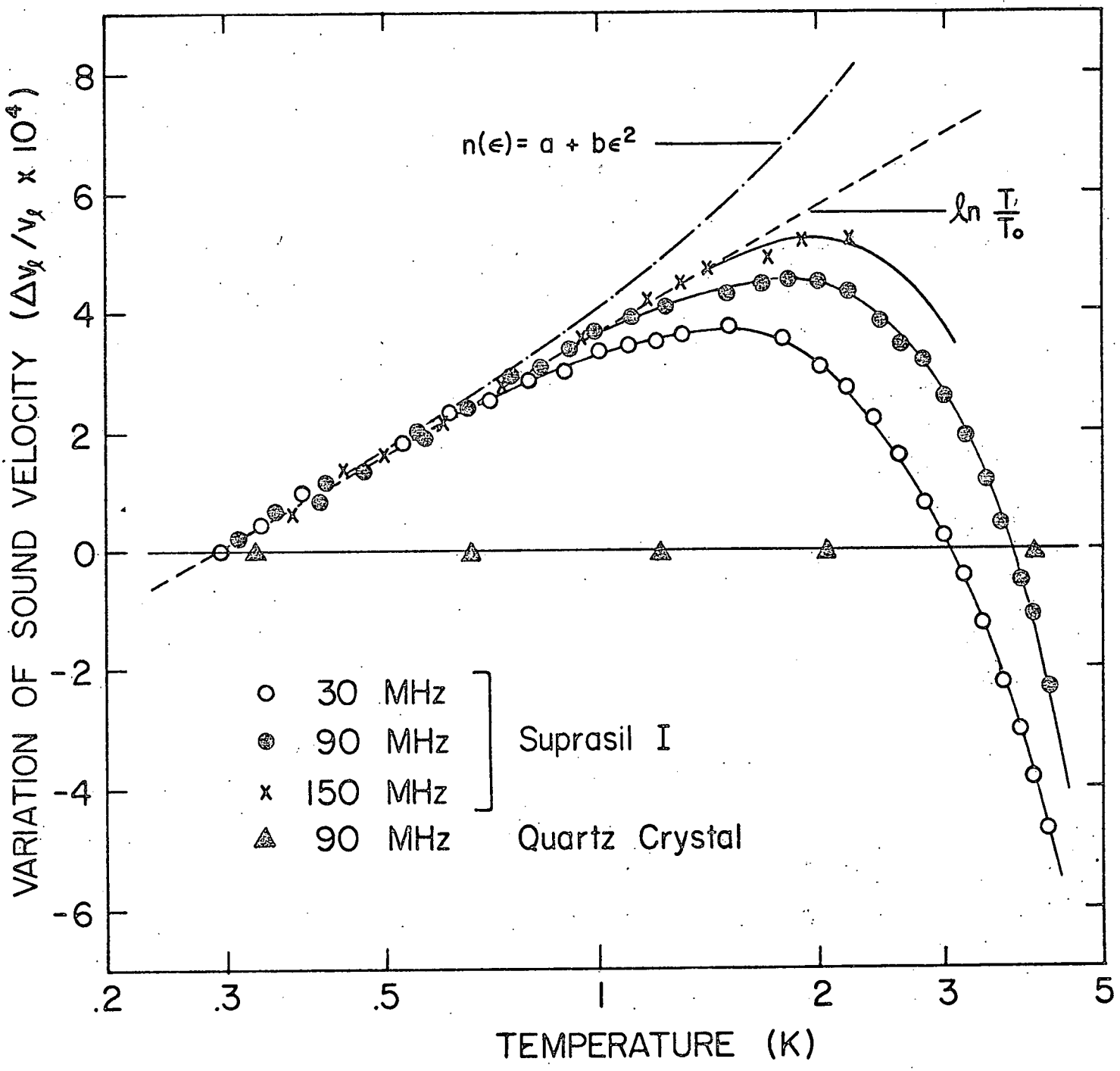
VARIATION OF SOUND VELOCITY ($\Delta v_t / v_t \times 10^4$)
8
6
4
2
0
-2
-4
-6
.2
.3
.5
1
2
3
5
TEMPERATURE (K)
$n(\epsilon) = a + b\epsilon^2$
$\ln \frac{T}{T_0}$
30 MHz
90 MHz
150 MHz
Suprasil I
90 MHz
Quartz Crystal

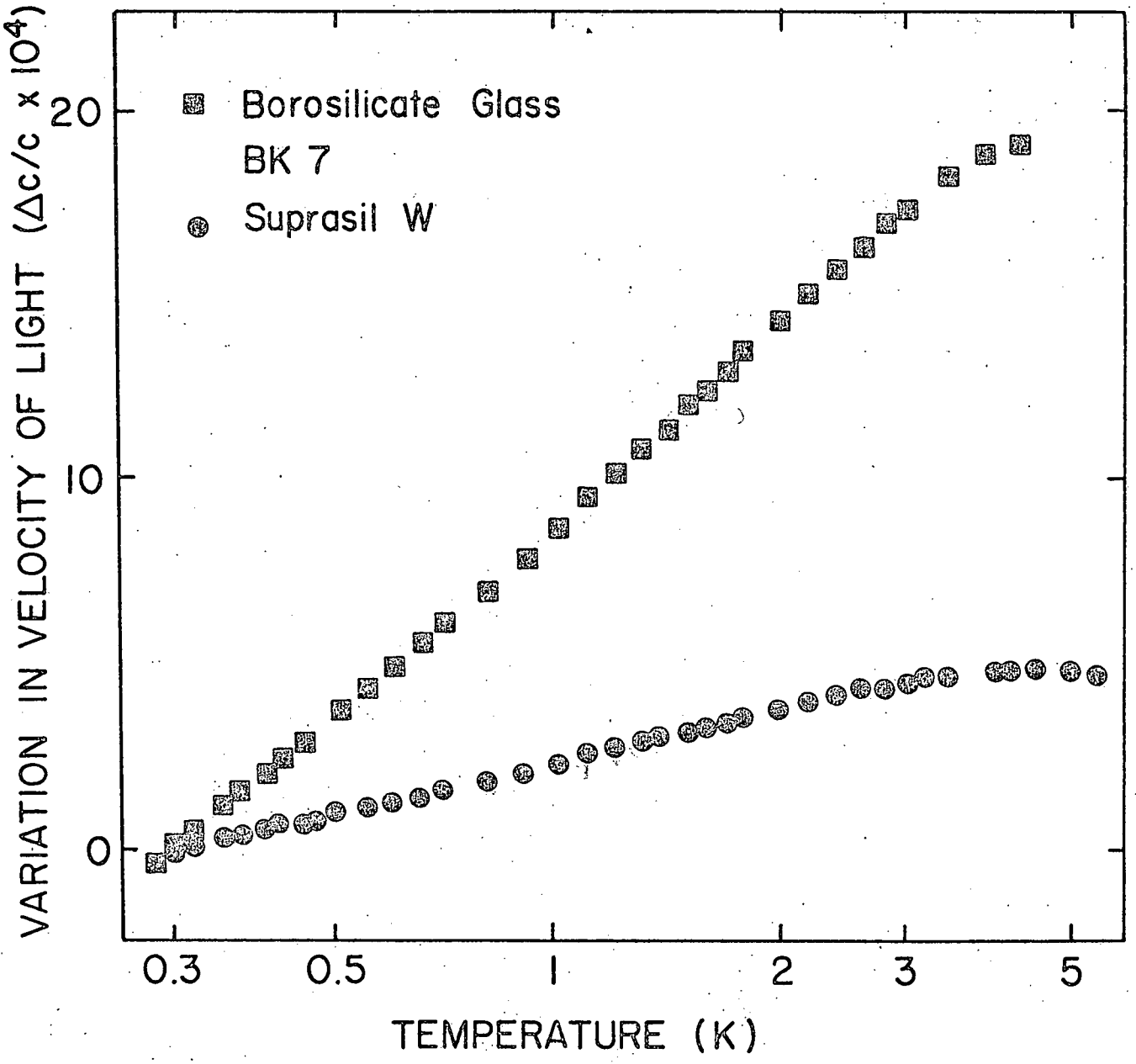
Borosilicate Glass
BK 7
Suprasil W
VARIATION IN VELOCITY OF LIGHT (Δc/c x 10⁴)
20
10
0
0.3
0.5
1
2
3
5
TEMPERATURE (K)

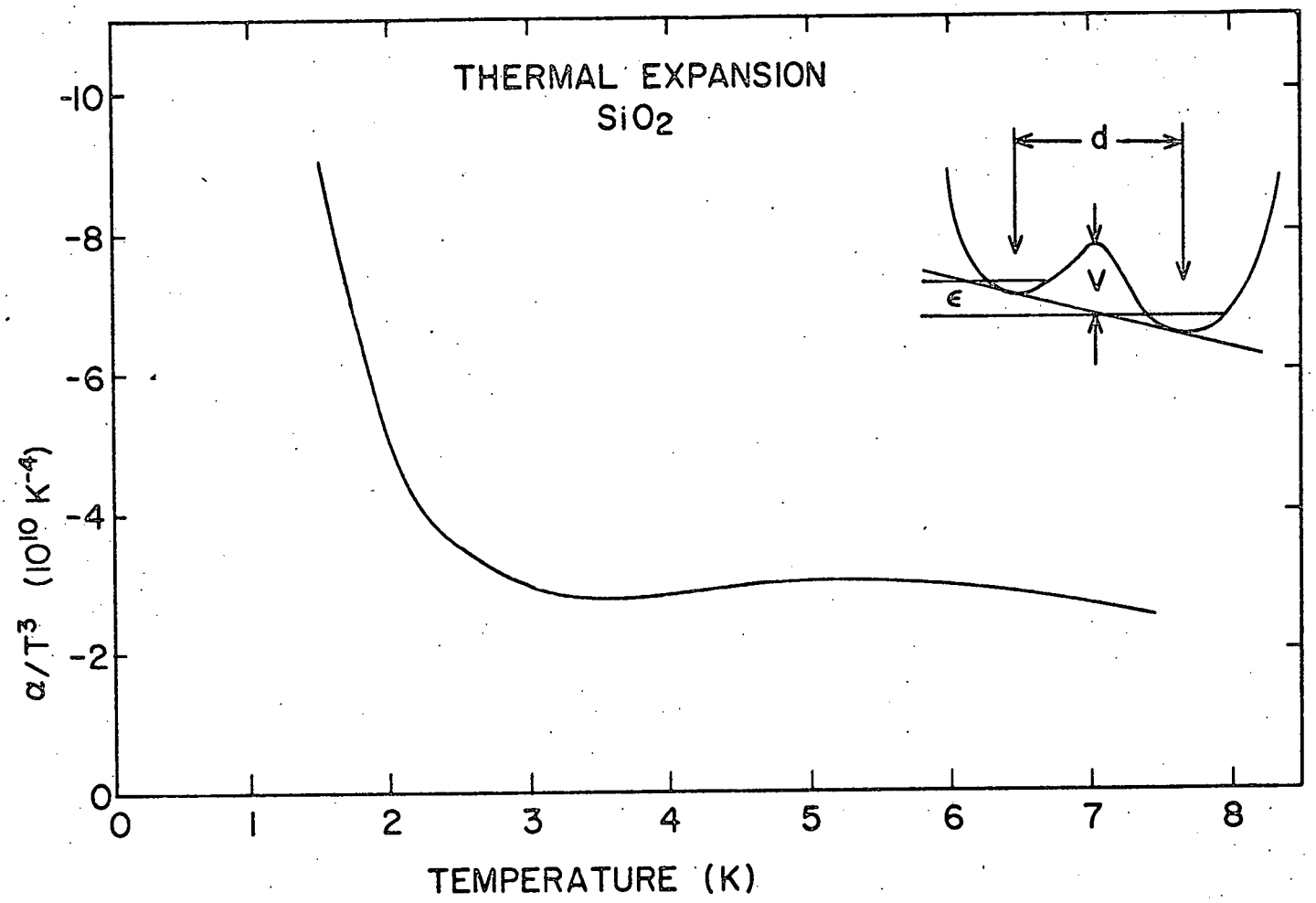
THERMAL EXPANSION
SiO2
d
V
ϵ
-10
-8
-6
-4
-2
0
0
1
2
3
4
5
6
7
8
α/T3 (10^10 K^-4)
TEMPERATURE (K)

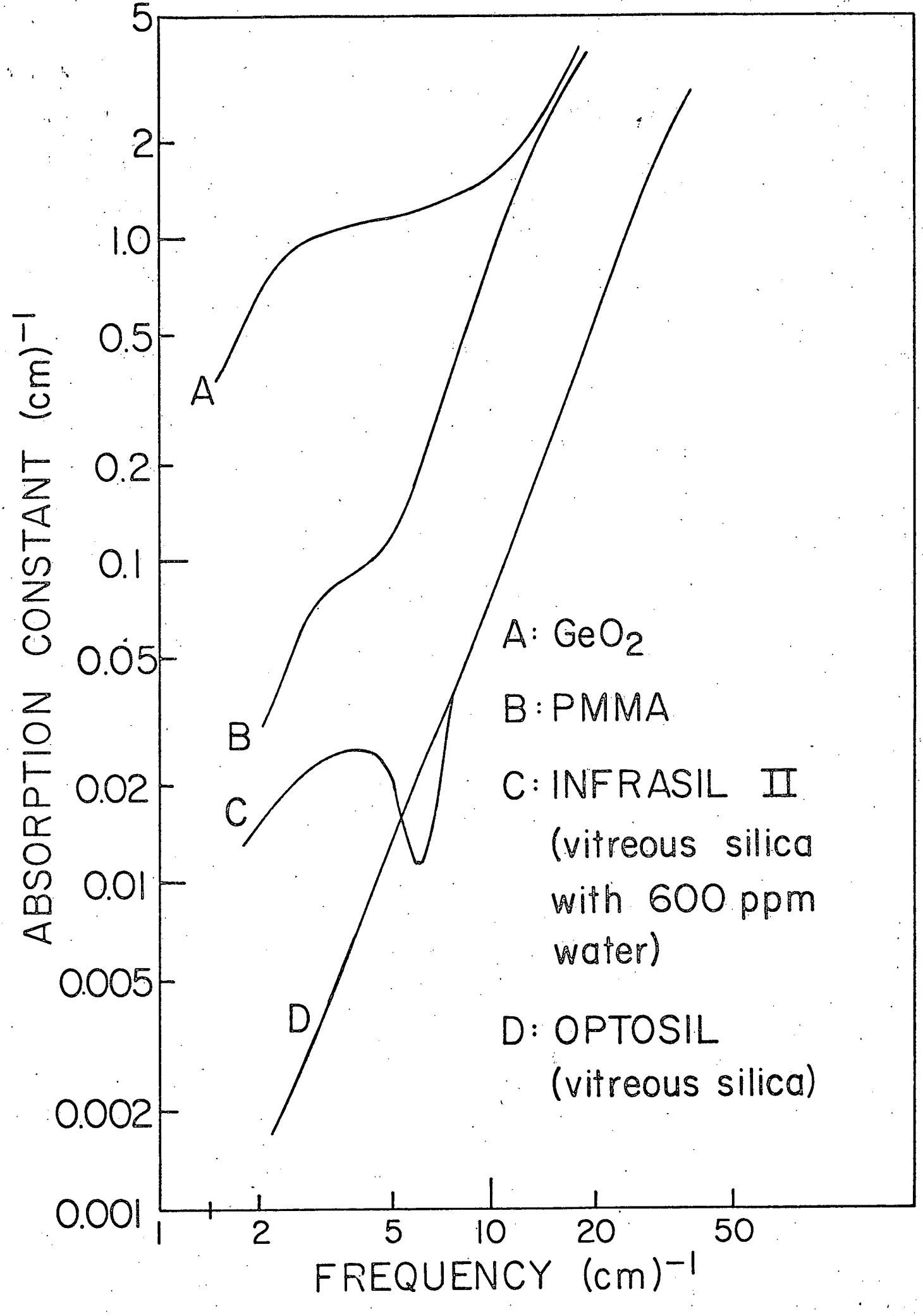
ABSORPTION CONSTANT (cm)⁻¹
5
2
1.0
0.5
0.2
0.1
0.05
0.02
0.01
0.005
0.002
0.001
1
2
5
10
20
50
FREQUENCY (cm)⁻¹
A
B
C
D
A: GeO2
B: PMMA
C: INFRASIL II
(vitreous silica
with 600 ppm
water)
D: OPTOSIL
(vitreous silica)

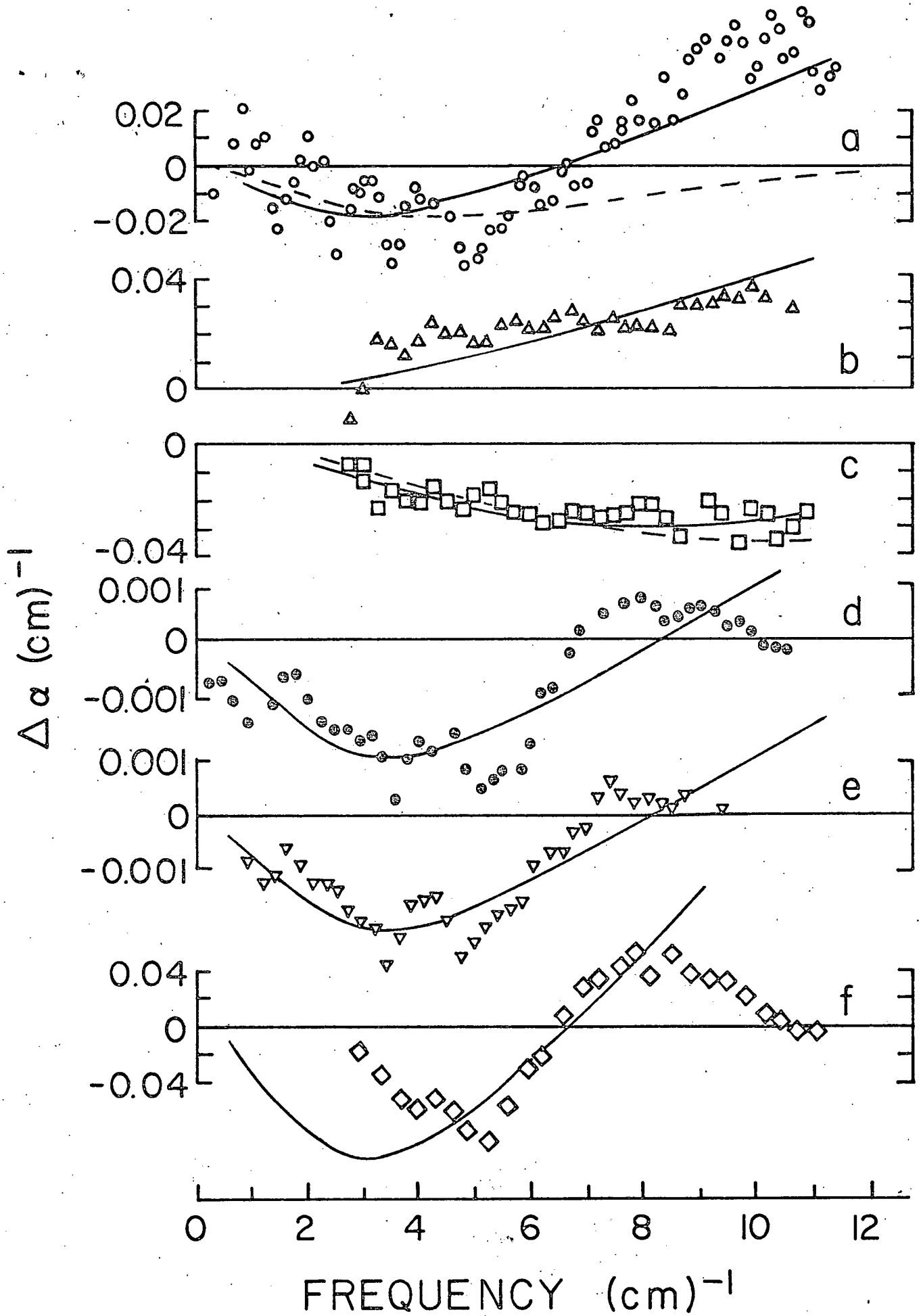
0.02
0
-0.02
a
0.04
0
b
0
-0.04
c
0.001
0
-0.001
d
0.001
0
-0.001
e
0.04
0
-0.04
f
Δα (cm)⁻¹
0
2
4
6
8
10
12
FREQUENCY (cm)⁻¹

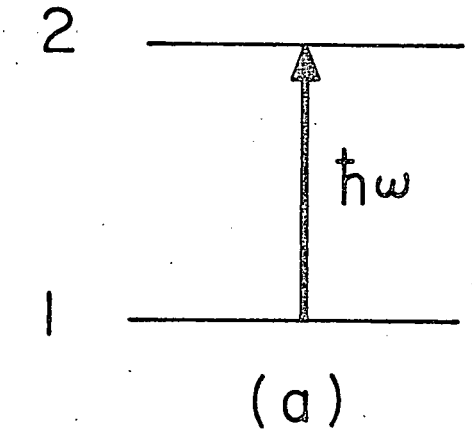

(a)

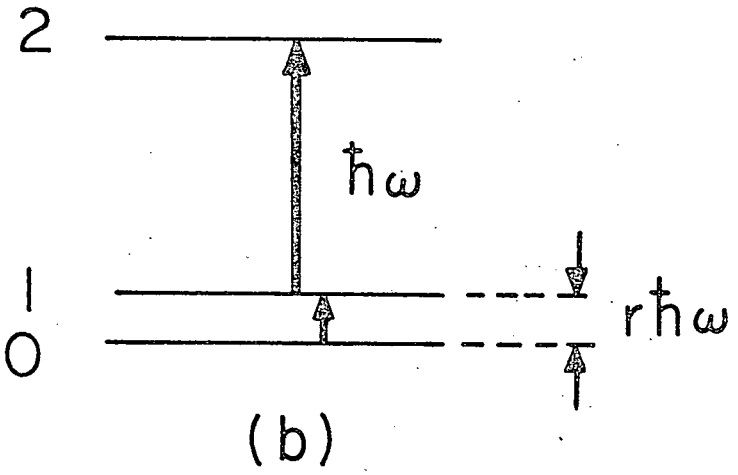

(b)

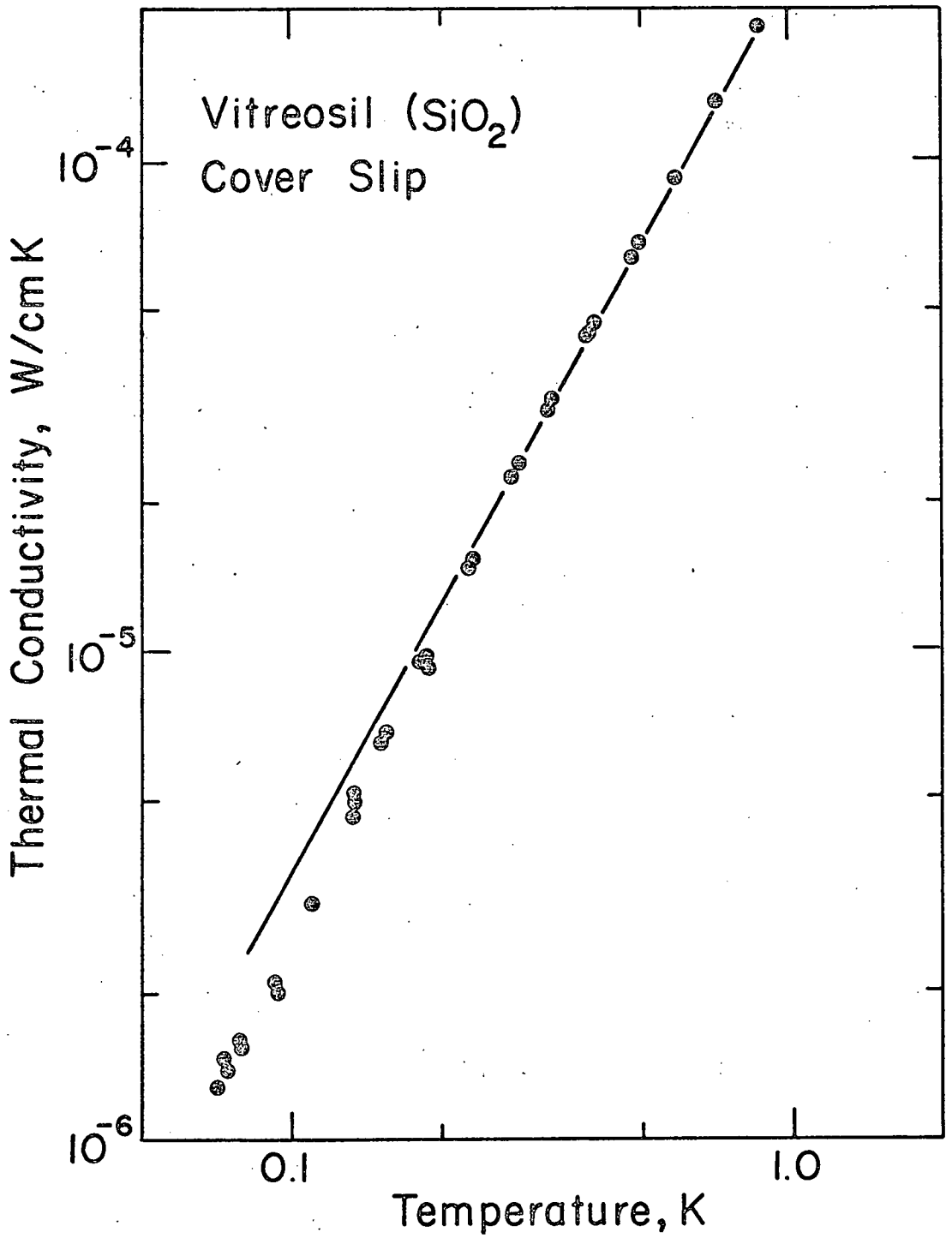
Vitreosil (SiO_2)
Cover Slip
10^{-4}
10^{-5}
10^{-6}
Thermal Conductivity, W/cm K
0.1
1.0
Temperature, K

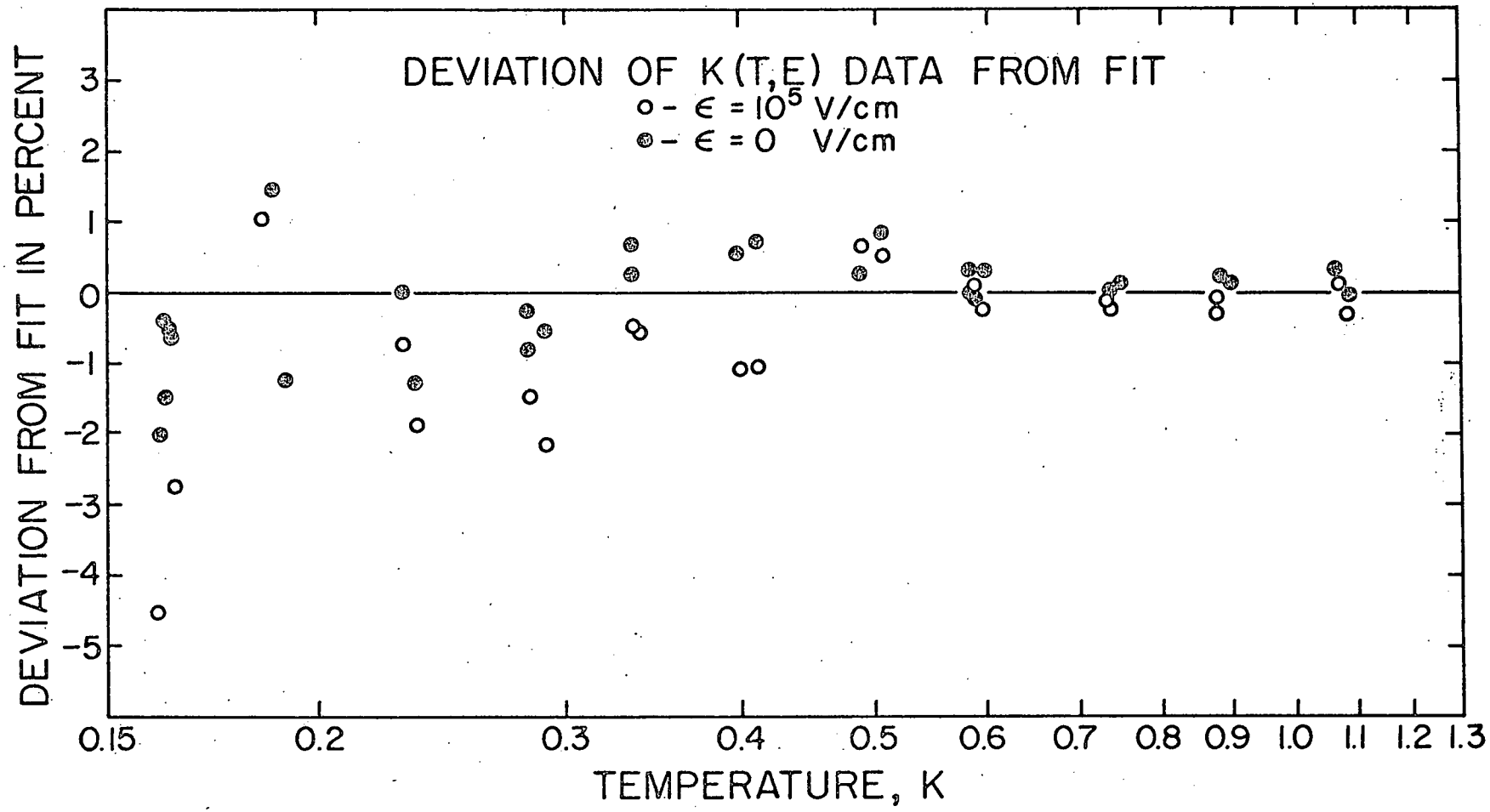
DEVIATION OF K(T,E) DATA FROM FIT
o - ∈ = 10^5 V/cm
⊙ - ∈ = 0 V/cm
DEVIATION FROM FIT IN PERCENT
3
2
1
0
-1
-2
-3
-4
-5
0.15
0.2
0.3
0.4
0.5
0.6
0.7
0.8
0.9
1.0
1.1
1.2
1.3
TEMPERATURE, K

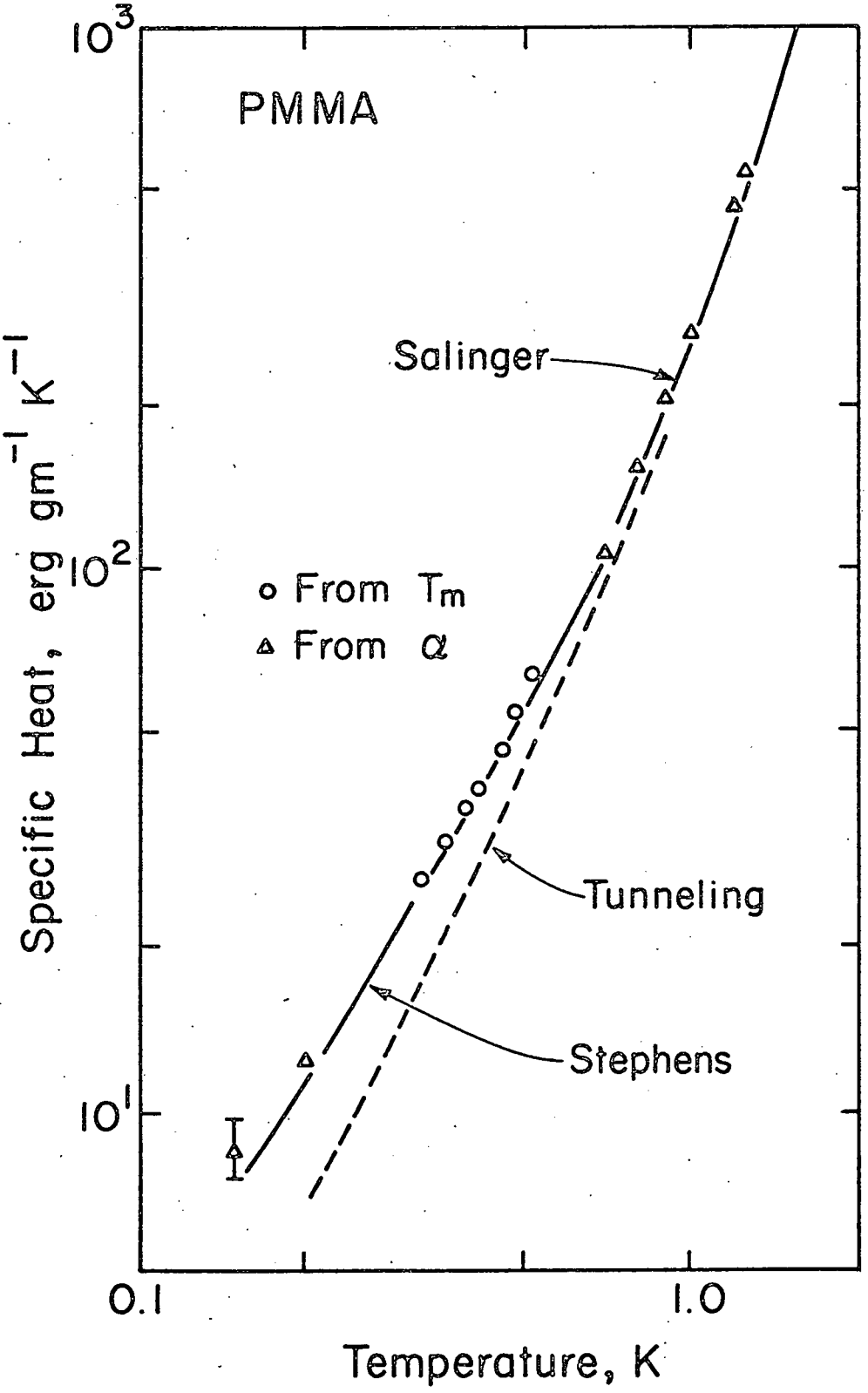
PMMA
Salinger
Tunneling
Stephens
From T_m
From α
Specific Heat, erg gm^{-1} K^{-1}
Temperature, K
10^3
10^2
10^1
0.1
1.0

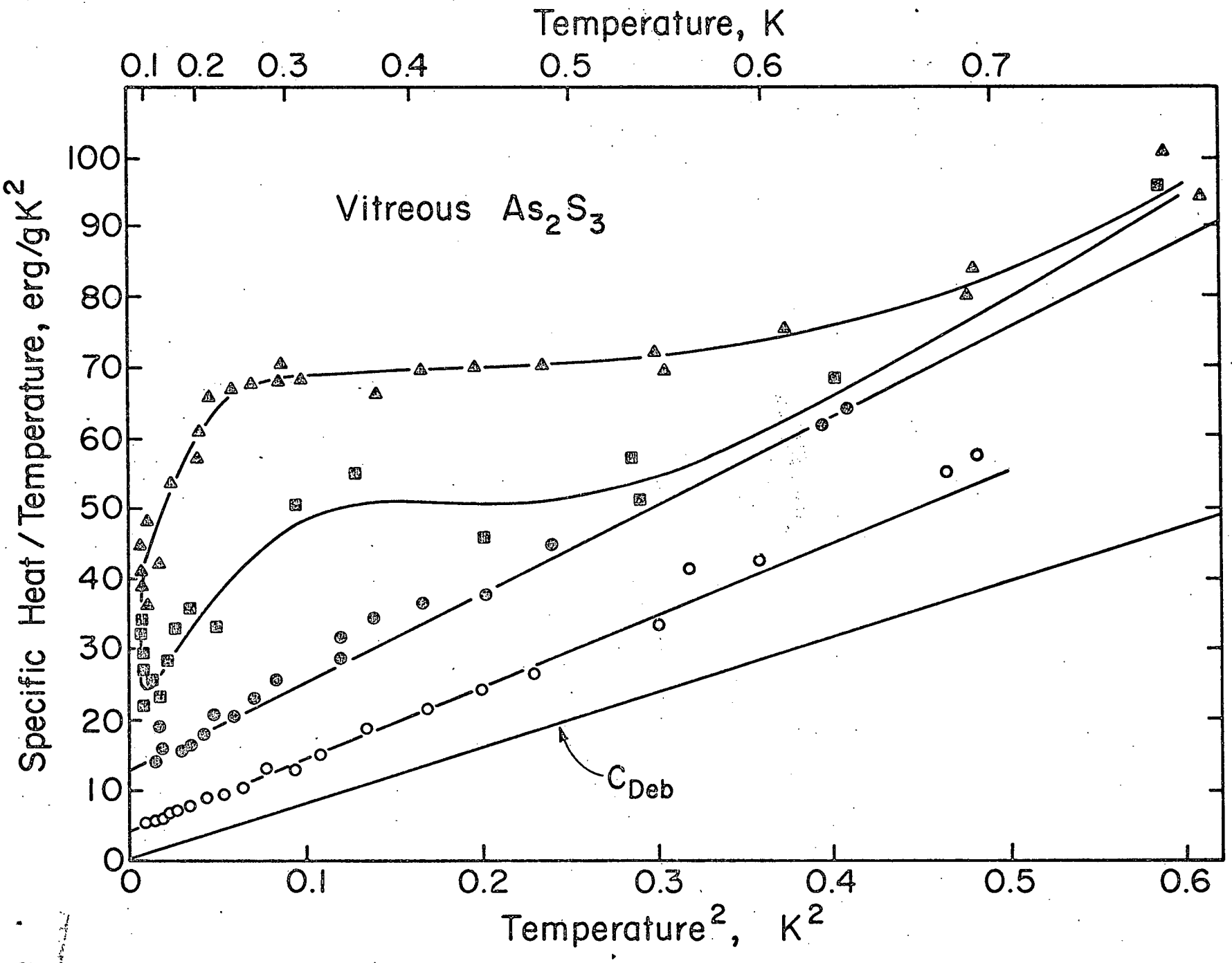
Temperature, K
0.1
0.2
0.3
0.4
0.5
0.6
0.7
Vitreous As_2S_3
Specific Heat / Temperature, erg/gK^2
100
90
80
70
60
50
40
30
20
10
0
C_{Deb}
0
0.1
0.2
0.3
0.4
0.5
0.6
Temperature^2, K^2

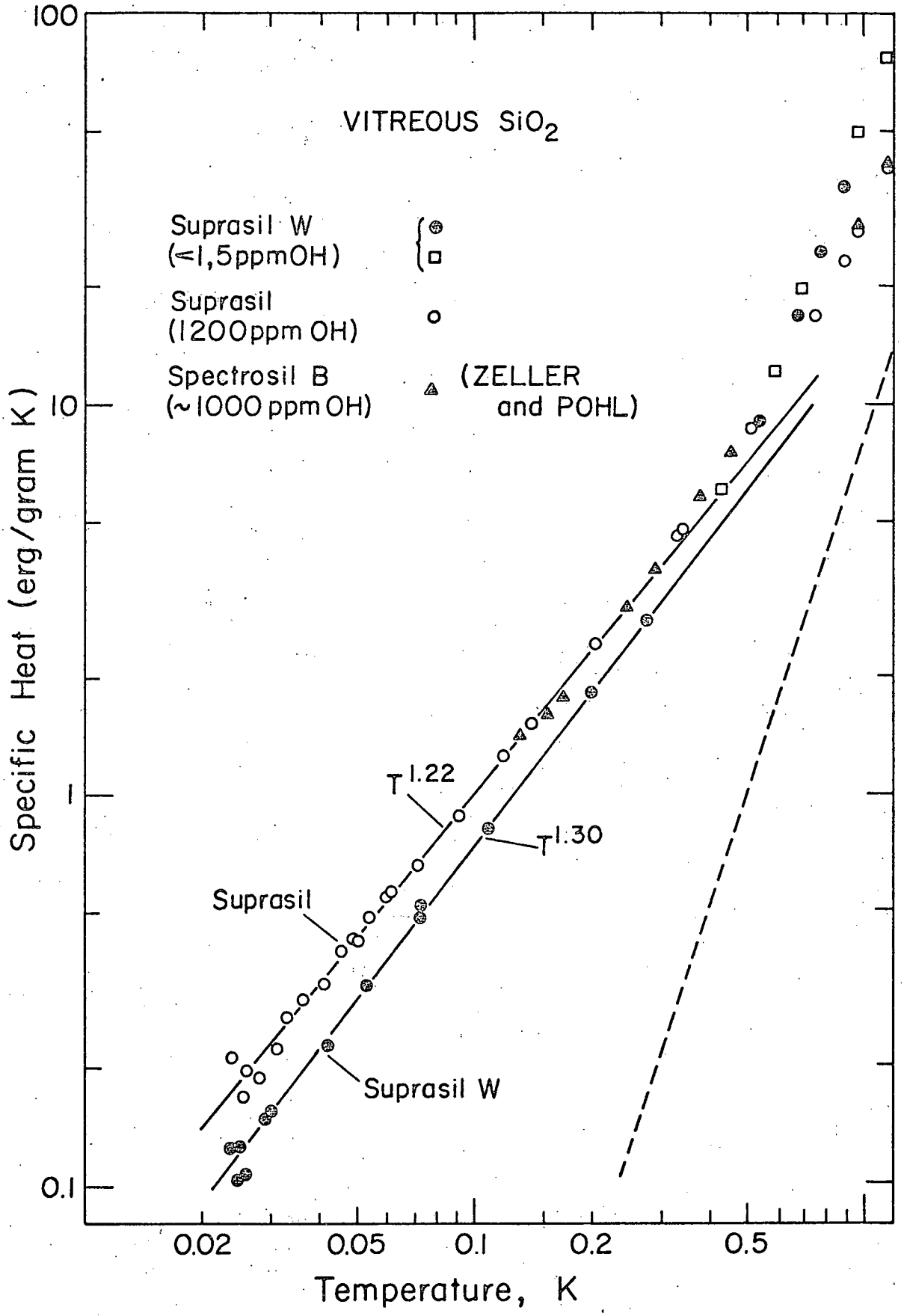
VITREOUS SiO_2
Suprasil W
(≤1,5ppmOH)
Suprasil
(1200ppm OH)
Spectrosil B
(~1000 ppm OH)
(ZELLER
and POHL)
$T^{1.22}$
$T^{1.30}$
Suprasil
Suprasil W
Specific Heat (erg/gram K)
Temperature, K
100
10
1
0.1
0.02
0.05
0.1
0.2
0.5

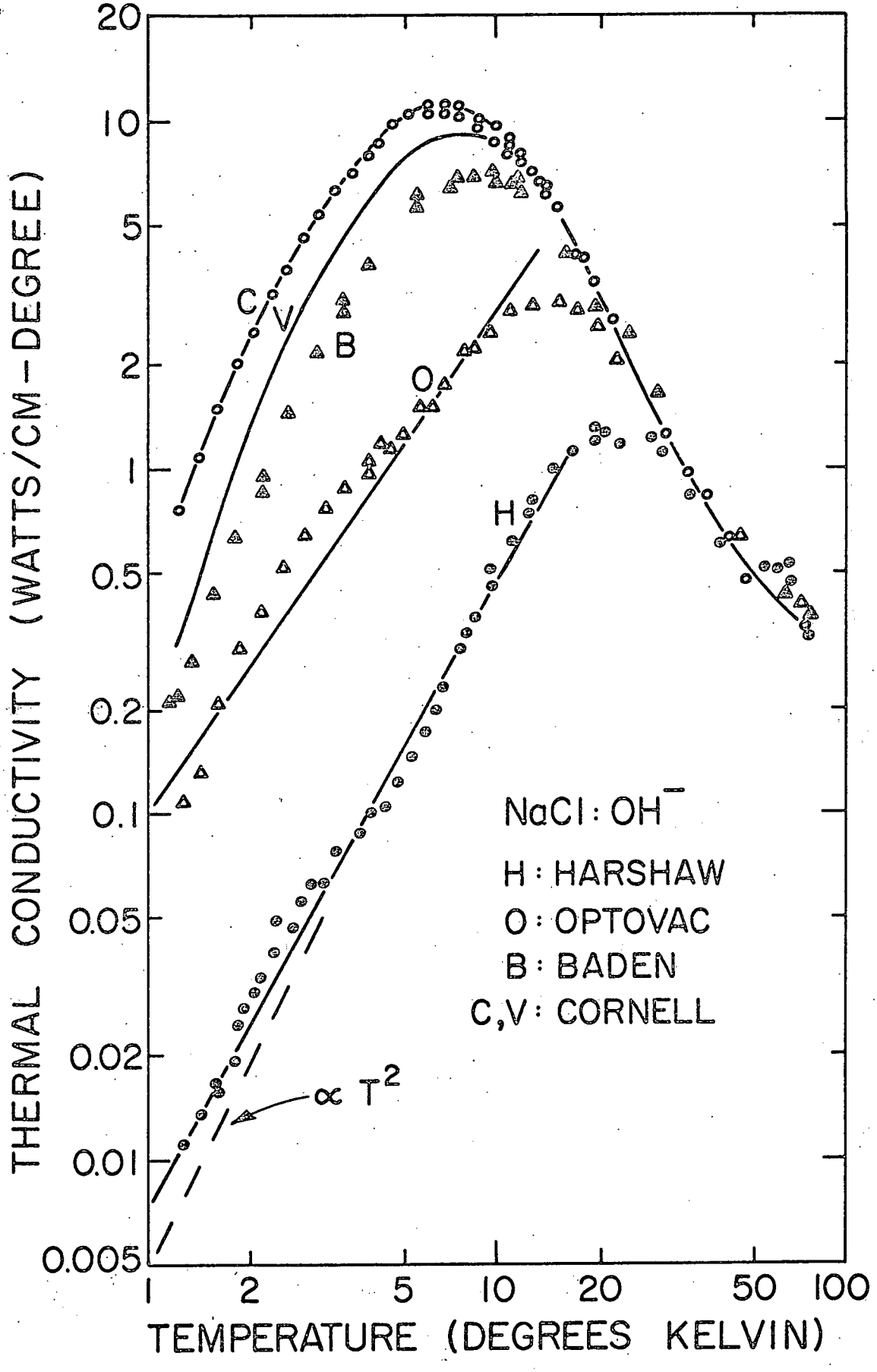
THERMAL CONDUCTIVITY (WATTS/CM-DEGREE)
20
10
5
2
1
0.5
0.2
0.1
0.05
0.02
0.01
0.005
1
2
5
10
20
50
100
TEMPERATURE (DEGREES KELVIN)
C
V
B
O
H
NaCl : OH⁻
H : HARSHAW
O : OPTOVAC
B : BADEN
C,V : CORNELL
∝ T²

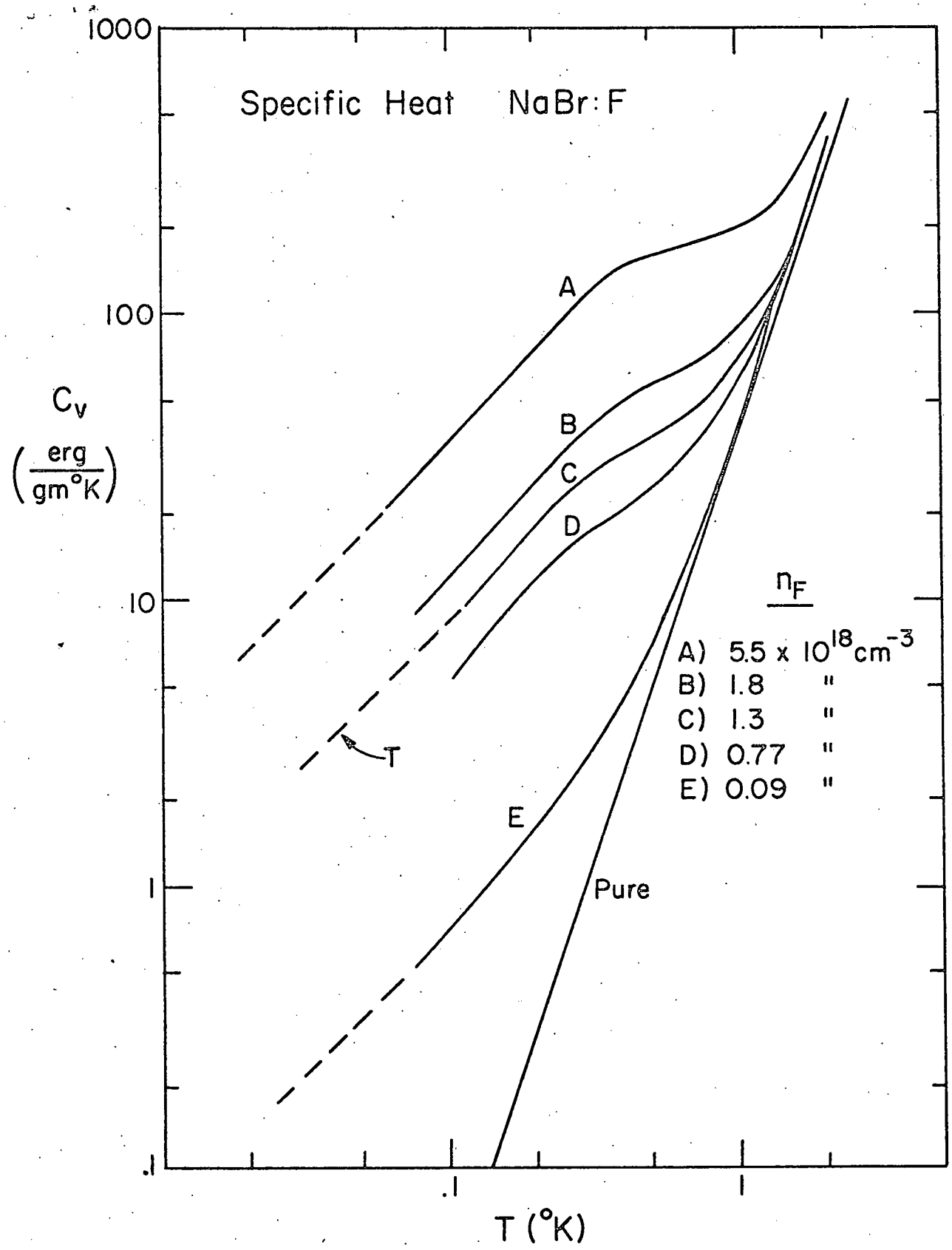
Specific Heat NaBr:F
1000
100
10
1
.1
C_v
$\left(\frac{erg}{gm°K}\right)$
A
B
C
D
E
Pure
T
n_F
A) 5.5 x 10^{18} cm^{-3}
B) 1.8 "
C) 1.3 "
D) 0.77 "
E) 0.09 "
.1
1
T (°K)